~~CONFIDENTIAL~~ UNCLASSIFIED

NASA CONTRACTOR REPORT

UB
NASA CR-276

NASA CR-276

FOR U.S. GOVERNMENT AGENCIES AND THEIR CONTRACTORS ONLY.

CLASSIFICATION CHANGED TO UNCLASSIFIED
By Authority of NASA lib. advt 3-75
Initial/Date Helen Wiener 4-8-75

# ANALYSIS OF SECONDARY-FLOW-CONTROL METHODS FOR CONFINED VORTEX FLOWS

*by Bruce V. Johnson*

Prepared under Contract No. NASw-847 *by*
UNITED AIRCRAFT CORPORATION
East Hartford, Conn.
*for*

NATIONAL AERONAUTICS AND SPACE ADMINISTRATION · WASHINGTON, D. C. · JANUARY 1966

~~CONFIDENTIAL~~ UNCLASSIFIED

UNCLASSIFIED
~~CONFIDENTIAL~~
FOR U.S. GOVERNMENT AGENCIES
AND THEIR CONTRACTORS ONLY.

NASA CR-276

# ANALYSIS OF SECONDARY-FLOW-CONTROL METHODS FOR CONFINED VORTEX FLOWS

By Bruce V. Johnson

CLASSIFICATION CHANGED
TO UNCLASSIFIED
By Authority of NASA ltr dtd 1-3-73
Initial/Date S/Howard G. Maines dkm 03/09

Distribution of this report is provided in the interest of information exchange. Responsibility for the contents resides in the author or organization that prepared it.

GROUP 4
Downgraded at 3 year intervals;
declassified after 12 years

CLASSIFIED DOCUMENT–TITLE UNCLASSIFIED
This material contains information affecting the national defense of the United States within the meaning of the espionage laws, Title 18, U.S.C., Secs. 793 and 794, the transmission or revelation of which in any manner to an unauthorized person is prohibited by law.

NOTICE
This document should not be returned after it has satisfied your requirements. It may be disposed of in accordance with your local security regulations or the appropriate provisions of the Industrial Security Manual for Safe-Guarding Classified Information.

Prepared under Contract No. NASw-847 by
UNITED AIRCRAFT CORPORATION
East Hartford, Conn.

for

NATIONAL AERONAUTICS AND SPACE ADMINISTRATION

UNCLASSIFIED
~~CONFIDENTIAL~~

**Page intentionally left blank**

UNCLASSIFIED

~~CONFIDENTIAL~~

Analysis of Secondary-Flow-Control Methods

for Confined Vortex Flows

TABLE OF CONTENTS

| | Page |
|---|---|
| SUMMARY | 1 |
| CONCLUSIONS | 1 |
| INTRODUCTION | 2 |
| FLOW MODEL | 4 |
| BOUNDARY LAYER CHARACTERISTICS WITHOUT SECONDARY-FLOW CONTROL | 5 |
| ANALYSIS OF SECONDARY-FLOW CONTROL | 5 |
| DISCUSSION OF RESULTS | 7 |
| Constant-Density Fluids | 7 |
| Variable-Density Fluids | 11 |
| REFERENCES | 14 |
| LIST OF SYMBOLS | 15 |
| APPENDIX - DERIVATION OF EQUATIONS FOR SECONDARY-FLOW CONTROL | 18 |
| TABLES | 26 - 28 |
| FIGURES | 29 - 54 |



~~CONFIDENTIAL~~

UNCLASSIFIED

UNCLASSIFIED
~~CONFIDENTIAL~~

# Analysis of Secondary-Flow-Control Methods for Confined Vortex Flows

## SUMMARY

An analysis was performed to determine criteria to prevent flow from the end-wall boundary layers (secondary flow) to the central region (primary flow) of a confined, cylindrical vortex. The secondary flow was analyzed by a boundary layer momentum-integral technique for cases in which primary-flow circulation $\Gamma$ (product of tangential velocity and local radius) is proportional to the radius to the $n_\Gamma$ power (i.e., $\Gamma \propto r^{n_\Gamma}$). Radial variations of local end-wall friction coefficient and end-wall suction were investigated as means to alter the radial distribution of angular momentum in the boundary layers and thereby to control the primary flow-secondary flow interactions.

The results of the analysis yield the radial variation of either local friction or wall suction which must be employed to prevent fluid transfer between the primary and secondary flows. The variation of boundary layer thickness with radius is also calculated. Results are obtained for: (1) a constant-density fluid with $n_\Gamma = 0.5$, 1, 2, 3, and 4, and (2) variable-density fluid with $n_\Gamma = 3$ and four different rates of axial mass transfer between the higher-density primary flow and the lower-density secondary flow.

## CONCLUSIONS

1. The magnitude of the friction or suction required to prevent convection from the secondary flow to the primary flow is a function of the quantity of flow within the end-wall boundary layer and the circulation distribution in the primary flow. In addition, the quantity of suction required is strongly dependent on the increased wall shear due to wall suction.

2. The effective tangential skin-friction coefficient required to eliminate convection from the secondary to the primary flow in a vortex tube increases with decreasing radius. The absolute value of friction coefficient at small radii may be several orders of magnitude larger than the naturally occurring skin-friction coefficient on smooth end walls.

~~CONFIDENTIAL~~
UNCLASSIFIED

3. The boundary layer thickness may increase to the same order of magnitude as the vortex tube radius when using distributed-friction end walls for secondary-flow control.

4. When utilizing distributed-suction end walls for secondary-flow control, a substantial portion of the radial flow initially in the end-wall boundary layer must be withdrawn through the suction end walls in order to eliminate convection from the end-wall boundary layer.

5. When using suction end walls for secondary-flow control, the boundary layer thickness is of the same or a smaller order of magnitude than that which occurs for plain end walls.

6. An increase in density in the primary flow with decreasing radius has no effect on either the friction or suction required to eliminate convection from the end-wall boundary layer if there is no axial diffusion between the primary and secondary flows.

7. An increase in density in the primary flow with decreasing radius will cause a decrease in end-wall boundary layer thickness if there is no axial diffusion or convection between the primary and secondary flows.

8. Axial diffusion of high-density fluid from the primary flow into low-density fluid in the secondary flow will lead to a relatively small increase in friction or suction required to eliminate convection from the secondary flow into the primary flow.

9. Axial diffusion of high-density fluid from the primary flow into low-density fluid in the secondary flow will cause a relatively small increase in end-wall boundary layer thickness for configurations in which there is no convection between the primary and secondary flows.

## INTRODUCTION

Determination of the feasibility of gaseous nuclear rocket concepts involving vortex flow for containment of nuclear fuel requires detailed knowledge of confined vortex characteristics over a wide range of conditions. Theoretical studies indicate that friction on the end walls of vortex tubes has a major influence on vortex-flow characteristics for flows of interest in such rocket concepts. According to theory, the radial velocities in the secondary-flow region (end-wall boundary layers) may be of the same order of magnitude as the tangential velocities in the primary-flow region (region outside the end-wall boundary layers) but orders of magnitude larger than the radial velocities in the primary-flow region. Secondary

flows are usually accompanied by axial velocities in the primary-flow region both into and out of the end-wall boundary layers at different radii.

The characteristics of a boundary layer on a flat plate with a specified rotating external flow have been analyzed previously by Mack (Ref. 1), King (Ref. 2), and others (see Refs. 1 and 2) utilizing momentum-integral techniques. Mack (Ref. 1) investigated the effect of various laminar velocity profiles on the radial boundary layer mass flow and found the flow rate to be rather insensitive to the assumed profile shape. King (Ref. 2) investigated several momentum-integral techniques and found good agreement between most of the methods.

Anderson (Refs. 3 and 4) investigated confined vortex flows and found very strong coupling between the primary and secondary-flow regions with a large amount of flow interchange for some flow conditions. Measurement of flow characteristics in confined vortex tubes by Owen, Hale, Johnson and Travers (Ref. 5), Kendall (Ref. 6) and Johnson, Travers and Hale (Ref. 7) substantiate the general characteristics of vortex flows predicted by theory for confined vortexes with turbulent end-wall boundary layers (Ref. 4). The axial velocities in the primary-flow region of the vortex tube are undesirable, when vortex flow is to be utilized for containment of nuclear fuel, since they cause convection of fuel from the rocket. A technique to reduce or eliminate these velocities is needed.

Since a secondary flow will form along a stationary wall adjacent to a rotating flow, convection toward the wall will always occur at some radii. Suggestions for preventing the flow from subsequently leaving the boundary layer at other radii have been made by Mack (Ref. 1), who proposed wall suction, and Johnson, Travers and Hale (Ref. 7). Results from a momentum-integral analysis in Ref. 7 indicated that increased friction by protrusions from the wall or by wall suction would be equally effective in preventing secondary flow from re-entering the primary flow. Both of these suggested techniques require that an established secondary flow exist at the outer radius of the region in which the axial flow is to be eliminated by secondary-flow control.

The objectives of the present investigation of secondary-flow control with distributed friction or distributed suction end walls were to extend the analysis of Ref. 7 (1) to include a modified friction coefficient due to suction, (2) to include boundary layer thickness calculations and (3) to determine the effect of axial mass transfer by diffusion of heavy gas from the primary flow to the secondary flow on the secondary-flow requirements for the case in which the primary-flow density is greater than the secondary-flow density.

## FLOW MODEL

The vortex tube geometry considered in the analysis is shown in Fig. 1. The peripheral wall of the vortex tube consists of a cylinder of length $L$ and radius $r_1$ through which flow is introduced with tangential velocity $V_{\phi,1}$ and radial velocity $V_{r,1}$. The ends of the vortex tube are annular plates with outside radius $r_1$ and inside radius $r_0$. Flow is withdrawn through the holes at the center of each plate. Because of the friction between the rotating flow and the end wall, a boundary layer develops on the end wall. The flow in the end-wall boundary layer and the flow in the central region of the vortex tube will be denoted secondary flow and primary flow, respectively. A sketch of the tangential and radial velocity distributions which occur in the primary and secondary-flow regions ($V_\phi$, $V_r$ and $U_\phi$, $U_r$, respectively) are shown in Fig. 2. The centrifugal acceleration of the primary flow due to its rotation is balanced by a radial pressure gradient. In the end-wall boundary layer the tangential velocities are reduced by shear on the plate; however, since pressure gradients normal to a boundary layer can usually be assumed negligible, the radial pressure gradient in the boundary layer can be assumed equal to the radial pressure gradient present in the primary flow. This radial pressure gradient accelerates the boundary layer flow inward to large radial velocities with the result that an appreciable amount of flow is convected into the boundary layer from the primary flow near the outer radius of the tube. At smaller radii, where the boundary layer flow is large, flow conditions may be encountered for which flow begins to leave the boundary layer and be convected into the primary flow.

In the vortex flows of interest in the present study, the flow is to be controlled so that there are regions in which no flow interchange takes place between the primary and secondary flows. For these regions the primary-flow tangential velocity distributions may be obtained from the well known solution of the Navier-Stokes equations for the case of constant radial flow rate between an outer radius $r_1$ and an inner radius $r_{10}$ with tangential velocities of $V_{\phi,1}$ and $V_{\phi,10}$, respectively, constant viscosity, and a radial velocity $V_{r,1}$ at $r_1$. For the condition with a line source or sink at the center ($r_{10} = 0$) and $V_{\phi,10} = 0$, the solution reduces to

$$\bar{\Gamma} = \frac{\Gamma}{\Gamma_1} = \frac{V_\phi r}{V_{\phi,1} r_1} = \left(\frac{r}{r_1}\right)^{n_\Gamma} = R^{n_\Gamma} \tag{1}$$

where $n_\Gamma = 2 - Re_{rp}$ and $Re_{rp} = -V_r r / \nu$. Equation (1) satisfies the above boundary conditions for $Re_{rp} < 1$. The variations of tangential velocity ratio, $V_\phi / V_{\phi,1}$ and circulation ratio, $V_\phi r / V_{\phi,1} r_1$ with radius ratio, $r / r_1$, have been evaluated from Eq. (1) and are presented in Fig. 3.

In Ref. 3, Anderson eliminated the assumption of a line sink and assumed that the radial flow per unit axial distance decreased parabolically with radius from the

uniform value outside of $r_{10}$ to zero at the centerline. For $Re_{rp} < 1$ and $r_{10} / r_1 = 0.1$, this method resulted in primary-flow tangential velocity distributions very close to those obtainable from Eq. (1). These results are shown in Fig. 3 for $Re_{rp} = 1$ and 3. Because of the good agreement between the results of Eq. (1) and the more exact solutions of Anderson for the small values of $Re_{rp}$ of interest in this report, the tangential velocity distributions required for calculation of secondary-flow-control requirements were obtained from Eq. (1).

## BOUNDARY LAYER CHARACTERISTICS WITHOUT SECONDARY-FLOW CONTROL

Anderson's computational program based on a momentum-integral analysis of a turbulent boundary layer on an annular plate (Ref. 4) was used to calculate the variation of secondary flow with radius for values of $Re_{rp}$ equal 3, 1, 0, -1, -2, and -4. The results which are presented in Fig. 4 are valid only for $L \to \infty$ because no changes in $Re_{rp}$ caused by flow into and out of the end-wall boundary layer are included in these calculations. The values of $Re_{rp}$ and $n_\Gamma$ are both noted on curves where solutions for the primary-flow circulation distribution are approximately equal for the Anderson model and $\bar{\Gamma} = R^{n_r}$. For a tangential velocity between $r_1$ and $r_{10}$ which corresponds to a free vortex ( $V_\phi r$ = constant, $n_\Gamma = 0$), the secondary flow ratio, $(-Q_s / 2\pi\nu r_1)\ Re_{t,1}^{-0.8}$, increases continuously with decreasing radius. For all of the other circulation distributions considered, the secondary-flow ratio increases with decreasing radius from $r_1$ until a maximum value is reached, then decreases to zero as $r$ approaches zero. The radius at which the maximum secondary flow occurs is denoted $r_6$. As the primary-flow radial Reynolds number $Re_{rp}$ decreases, the maximum amount of secondary flow decreases and the radius ratio at which this maximum occurs, $r_6 / r_1$, increases.

The variations of a dimensionless boundary layer thickness with radius for the secondary flows shown in Fig. 4 were calculated and the results are presented in Fig. 5. Note that for values of $Re_{rp} \leq 3$ the maximum boundary layer thickness occurs at a greater radius than the radius of maximum secondary flow, $r_6$ (denoted by the small arrows).

## ANALYSIS OF SECONDARY-FLOW CONTROL

The tangential momentum boundary layer equation can be used to develop criteria for the condition of no fluid transfer between the primary and secondary-flow regions. Consider the following form of the tangential-momentum integral equation (see, for example, Ref. 1) for a constant-density fluid with the assumptions outlined in Table I.

$$\rho_s \frac{d}{dr} \int_0^{\delta} (2\pi r U_r)(r U_\phi)\, dZ = -\rho_s (2\pi r U_{z,\delta})(r V_\phi) - \rho_s C_{ft} \pi r^2 V_\phi^2 \qquad (2)$$

where $C_{ft}\rho_s V_\phi^2 / 2$ is the tangential shear stress on the wall. The first term on the right side is the angular-momentum flux (per unit radius) between the secondary flow and the primary flow due to flow $(2\pi r U_{z,\delta})$ entering or leaving the end-wall boundary layer. The second term on the right side is the rate of angular momentum decrease in the boundary layer (per unit radius) due to end-wall skin friction. These two terms on the right side of Eq. (2) equal the radial gradient of angular momentum flux in the boundary layer.

To eliminate axial velocities in some region of the primary flow, it is necessary to eliminate the axial velocities at the edges of the end-wall boundary layers adjacent to this region $(U_{z,\delta} = 0)$. In this case, the first term on the right side of Eq. (2) becomes zero and the radial gradient of the angular momentum flux in the boundary layer must then equal the local torque due to end-wall skin friction. This condition is satisfied without the use of secondary-flow control at the radius marked $r_6$ on the secondary-flow-rate curves shown in Fig. 4.

The following form of Eq. (2), for the condition of a constant-density fluid and $U_{z,\delta} = 0$, is derived in the Appendix in terms of $Q_s$, the local secondary flow in one end-wall boundary layer, $\Gamma$, the local circulation and $K_7$, a coefficient which is a function of the shape of the boundary layer velocity profiles and which is defined in Table II. (The parameter $K_7$ has been assumed constant in all calculations discussed in the present report.)

$$\frac{d}{dr}\left[Q_s \Gamma K_7\right] = -C_{ft} \pi \Gamma^2 \qquad (3)$$

From Fig. 4 it can be seen that unless the secondary flow is artificially controlled, the secondary flow will decrease for $r < r_6$. To prevent axial flow by making $U_{z,\delta} = 0$, Eq. (3) must be satisfied at all radii less than $r_6$.

For a given circulation level $(\Gamma_6)$ at radius $r_6$ (where $dQ_s/dr$ is zero), the secondary flow is inversely proportional to the circulation gradient $(d\Gamma/dr)_6$ and $K_7$ and is directly proportional to $C_{ft}$.

$$Q_{s,6} = \frac{-C_{ft} \pi \Gamma_6^2}{K_7} \frac{1}{(d\Gamma/dr)_{r_6}} \qquad (4)$$

The variation of $d\Gamma/dr$ (nondimensionalized by the values of $\Gamma$ and $r$ at $r_6$) with radial Reynolds number is shown in Fig. 6 for the circulation profiles

$\Gamma = R^n r$ , and the circulation profiles calculated from the computational program of Ref. 3 (see Fig. 3 for the corresponding circulation profiles). The $(d\bar{\Gamma}/dR)_6$ curves evaluated on the basis of the two different assumptions coincide for $Re_{rp} < 1.0$ and diverge markedly for $Re_{rp} > 1$ , where the model for which $\bar{\Gamma} = R^n r$ loses its physical significance.

Two secondary-flow-control techniques will be analyzed, both of which entail increasing the skin-friction coefficient, $C_{ft}$ . In the first, a constant value of $Q_s$ in the end-wall boundary layer at all radii less than $r_6$ is assumed, and the resulting skin-friction coefficient distribution which must be provided (by roughening the wall or by protrusion from the wall) to prevent axial flow from the boundary layer is evaluated from Eq. (3). The second technique employs end-wall suction and $Q_s$ is then variable. Analysis of flat-plate flows (Ref. 8) indicates that the skin friction can be increased substantially by wall suction. For this analysis with rotating flow, the friction coefficient is assumed to be the sum of a flat-plate coefficient and a modified asymptotic suction coefficient.

$$C_{ft} = C_{ft,0} + \xi \, 2 U_{z,w} / V_\phi \qquad (5)$$

where $\xi$ is a parameter indicating the effectiveness of wall suction in increasing the skin friction. A summary of the parameters employed in analyzing the secondary-flow-control requirements is presented in Table III.

## DISCUSSION OF RESULTS

### Constant-Density Fluids

The primary condition imposed upon the solutions for the end-wall boundary layer characteristics is that no convection occur between the primary and secondary-flow regions (i.e., $U_{z,\delta} = 0$ ). Several primary-flow velocity distributions and secondary-flow rates at the radius $r_6$ (where flow control is initially applied), were considered and the conditions necessary for secondary-flow control were obtained. The boundary layer characteristics with secondary-flow control are compared to those shown previously for several primary-flow tangential velocity distributions with no flow control.

#### Distributed Friction

From Eq. (A21), the condition which must be satisfied to prevent flow interchange between the primary and secondary-flow regions and thus maintain constant radial flow in the end-wall boundary layer from $r_6$ to $r = 0$ $(1 \geq R \geq 0)$ is that

$$\frac{1}{\bar{\Gamma}^2}\frac{d\bar{\Gamma}}{dR} = C_{ft}\,J \tag{6}$$

where $J$ is given by

$$J = \frac{Re_{t,6}}{2S_6 K_7} \tag{7}$$

The skin-friction coefficient ratio, $C_{ft}/C_{ft,6}$, required to maintain a constant secondary flow is shown in Fig. 7 for four primary-flow circulation distributions corresponding to $\bar{\Gamma} = R^{n_\Gamma}$ where $n_\Gamma = 1, 2, 3,$ and $4$. A skin-friction distribution calculated on the basis of a circulation profile for $Re_{rp} = 1$ (Fig. 3) evaluated from the computation program of Ref. 3 is also presented for comparison. The results from the two methods are nearly identical for $Re_{rp} = 1$ and are identical for the other values of $Re_{rp}$ noted on Fig. 7. Note that the friction coefficient may have to increase by two to three orders of magnitude between $R = 1.0$ and $0.1$ to maintain a constant boundary layer flow; the weaker the vortex (i.e., the larger the value of $n_\Gamma$), the larger will be the change in $C_{ft}$ between these radii.

The effect of changes in $S_6$, the dimensionless initial flow in the end-wall boundary layer at radius $r_6$, on the variation of boundary layer thickness with radius is given in Fig. 8 for a specified vortex tube size. The corresponding values of $C_{ft,6}$ were evaluated from Eq. (6). (Note that for a selected primary-flow tangential velocity distribution and a fixed value of $Re_{t,6}$, the tangential skin-friction coefficient at $r_6$ is proportional to the radial flow $S_6$.) Values of the boundary layer thickness $\delta_6$ at $r_6$ compatible with these initial values of $S_6$ and $C_{ft,6}$ were then estimated on the basis of results similar to those shown in Fig. 5. Other reasonable assumptions might also have been made which would have yielded different $\delta_6$ values but the resulting differences in the boundary layer thickness at $r_6$ would not alter significantly the variation of boundary layer thickness with radius for $r < r_6$.

Within the boundary layer, the radial pressure gradient tends to increase the radial momentum (velocity) hence decreasing $\delta$ for a constant mass flow, while the radial skin friction tends to decrease the radial momentum and counteract the effect of the pressure gradient. If the radial momentum of the secondary flow were constant inside of $r_6$, the boundary layer thickness would increase as $1/r$. The result of the combined effects of the pressure gradient and skin friction for small values of $r$ is that the radial friction dominates and the boundary layer thickness actually increases faster than $1/r$. For the thick boundary layer shown by the upper curve in Fig. 8, $\delta$ increases continuously with a decrease in radius. For the thinner boundary layers shown by the lower curves, $\delta$ first decreases with a

decrease in radius and then increases. The calculated boundary layer thicknesses tend to be of the order of the tube radius for small values of $r$. Consequently, the boundary layer assumptions are not valid and the calculations are not accurate for small radii. However, it can be deduced from the results that very thick boundary layers will develop with this method of flow control.

Distributed Suction

The skin-friction coefficient $C_{f_t}$ is assumed to be the sum of a flat-plate skin-friction coefficient and an undetermined factor $\xi$ times the asymptotic suction skin-friction coefficient, $2 U_{z,w} / V_\phi$ (see Eq. (5)). It is shown in the Appendix (see Eq. (A26)) that $\xi$ must always exceed $K_7$ if end-wall suction is to result in a decrease in the average angular momentum (per unit mass) of the secondary flow. ($K_7$ is the ratio of the average angular momentum of the secondary flow at a given radius to the angular momentum this flow would have if it had the primary-flow tangential velocity.) If this condition is not satisfied, fluid having low angular momentum must be added to the boundary layer by wall blowing to prevent outflow from the boundary layer. For all of the calculations reported herein the ratio $\xi / K_7$ is assumed to be greater than unity.

In evaluating the effectiveness of secondary-flow control by suction, the three significant parameters in the governing equation ($n_\Gamma$, which describes the primary-flow circulation distribution, $\xi/K_7$ and $S_6$, the initial secondary-flow rate at $r_6$) have been systematically varied independently. To evaluate the influence of circulation distribution on the wall suction required to prevent flow between the primary and secondary-flow regions, five primary-flow circulation distributions were studied corresponding to $n_\Gamma = 0.5$, 1.0, 2.0, 3.0 and 4.0. The secondary flow at $r_6$ was assumed to be such that the radial gradient of angular momentum flux was equal to the decrease in angular momentum caused by the tangential skin friction (i.e., $C_{f_{t,6}} = C_{f_{t,0}} = 0.005$). A value of $\xi / K_7 = 1.1$ was selected for this calculation procedure.

The effect of circulation distribution on the ratio of the suction velocity to the tangential velocity at radius $r_6$ is shown in Fig. 9. The wall suction velocity increases continuously with a decrease in radius when the primary-flow tangential velocity $V_\phi$ increases with a decrease in radius ($n_\Gamma < 1$). However, this velocity first increases rapidly and then decreases with decreasing radius when $V_\phi$ decreases with a decrease in radius ($n_\Gamma > 1$). For the five cases studied the velocity ratio based on the local tangential velocity $V_\phi$ (see Fig. 10) increases from zero at $r_6$ to a fairly constant value within the central region of the vortex.

The variations of secondary-flow rate with radius which result from the suction distributions of Figs. 9 and 10 are shown in Fig. 11. Note that all of the $\bar{S}$ curves have zero slope at $R = 1$. A larger fraction of the radial flow initially in the boundary layer at $r_6$ is removed near that radius for large values

of $n_r$ (radial flow outward in the primary flow) and a larger fraction of the initial flow is retained in the end-wall boundary layer at small radii for small values of $n_r$ (radial flow inward in the primary flow).

Curves illustrating the effect of primary-flow circulation distribution on boundary layer thickness are shown in Fig. 12 for a particular tube size, tangential Reynolds number and value of $C_{ft,o}$. The boundary layer thicknesses at $r_6$ for each circulation distribution are compatible with the flow rate required at $r_6$ to ensure that $U_{z,\delta} = U_{z,w} = 0$. For primary-flow circulation distributions with radial flow outward ($n_r > 2$), where most of the secondary flow is removed near $r_6$, the boundary layer becomes thin at radii relatively near $r_6$. For cases where a substantial portion of the flow still remains in the boundary layer at small radii ($n_r < 1$), the boundary layer thins much more gradually with a decrease in radius. Note that in contrast to the distributed friction example (Fig. 8), the boundary layer thickness is always a small fraction of the dimensions of the tube (i.e., $\delta << r_6$).

In the previous calculation a value of $\xi / K_7 = 1.1$ was employed. The effect of several different values of $\xi / K_7$ on the end-wall suction requirements has been determined for a primary flow with solid-body rotation. The effect of $\xi / K_7$ on the wall-to-local tangential velocity ratio is shown in Fig. 13 for values of $\xi/K_7$= 2.0, 1.5, 1.25, 1.10 and 1.01. Corresponding secondary-flow rates are presented in Fig. 14. These results indicate that when a given suction velocity yields a large skin-friction coefficient (i.e., a large $\xi / K_7$ value), a larger fraction of the boundary layer flow remains at smaller radii than for values of $\xi / K_7$ close to 1.0. This is as one might expect since if suction does not effectively increase the skin friction, most of the boundary layer must be removed rapidly whereas, if small amounts of suction provide large increases in skin friction, more of the flow can remain in the boundary layer.

The effect of the wall suction parameter, $\xi / K_7$, on the variation of boundary layer thickness with radius is presented in Fig. 15. For $\xi / K_7 = 2.0$, the variation of boundary layer thickness with radius is similar to that found with distributed friction (see Fig. 8) since more of the flow remains in the boundary layer at large radii. When the suction is less effective, however, so that more of the flow is withdrawn near $r_6$, then the boundary layer thins continuously with a decrease in radius.

The characteristics of a flow in which the radial gradient of angular momentum equals the angular momentum loss due to tangential skin friction at $r_6$ have been discussed in preceding paragraphs. This condition represents the minimum secondary-flow rate which can exist at $r_6$ and is denoted as the reference flow. Now consider a secondary flow at $r_6$ which is greater than the reference flow. The increased friction required to prevent convection between the primary and secondary-flow regions can be obtained by wall suction at radius $r_6$. To illustrate this situation, the boundary layer characteristics have been analyzed for a primary flow with

solid-body rotation ($n_\Gamma = 2$) and two, four and ten times the reference flow in the boundary layer at radius $r_6$. The resulting variations with radius of the ratio of the flow in the end-wall boundary layer to the reference flow are presented in Fig. 16. Note that flow must be removed from the boundary layer at a greater rate between $R = 1$ and $R = 0.8$ for the flow conditions where $\bar{S}$ is greater than the reference flow rate. The $\xi/K_7$ value for these calculations was 1.1; for a larger value of $\xi/K_7$, some of the excess flow could remain in the end-wall boundary layer over a larger range of radii. For a value of $\xi/K_7$ closer to 1.0, the excess flow would have to be removed even closer to the radius at which suction was initially applied.

The variation of boundary layer thickness with radius is illustrated in Fig. 17 for the conditions at $r_6$ employed in the preparation of Fig. 16. Initial boundary layer thicknesses, compatible with the assumed flow rates, were estimated for each radial flow rate. Note that the boundary layer thicknesses decrease from the initial values at $r_6$ to a common value at a radius of approximately 3 in.

## Variable-Density Fluids

A confined vortex flow with a primary-flow radial density gradient at radii less than $r_6$ is analyzed in the following sections to determine the effect of this density gradient on the secondary-flow-control requirements. The secondary flow at $r_6$ is assumed to have the density of the primary flow at that radius. Diffusive mass transfer is allowed between the primary and secondary flows with two forms of the mass-transfer coefficients used to describe the mass-transfer process (discussed in the Appendix).

A time constant $t_{SF}$ (defined as the ratio of the mass of heavy gas contained in the vortex tube inside of $r_6$ to the rate at which the heavy gas is lost to the secondary flow) is evaluated. This time constant is then made nondimensional by dividing by $r_6^2/\nu$. Time constant results have been evaluated since the time constant is one of the important parameters which determine the suitability of a vortex flow for containment of nuclear fuel in a gaseous core nuclear rocket.

### Distributed Friction

The variation of the primary-flow density ratio, $\bar{\rho}_p$, with radius assumed in all calculations and the corresponding variation of the secondary-flow density ratio, $\bar{\rho}_s$, with radius for several axial-mass-transfer coefficients are shown in Fig. 18. The secondary-flow density ratio $\bar{\rho}_s$ for $h_d = 0.1\, V_\phi$ lies very close to the $\bar{\rho}_p$ curve at $R > 0.5$ but the difference between the curves increases with decreasing radius. The increase of $\bar{\rho}_s$ with decreasing radius is less for smaller values of $h_d$. The effect of a constant mass-transfer coefficient, $h_d = 0.01\, V_{\phi,6}$, is also shown in Fig. 18.

The tangential-skin-friction coefficient distribution required to prevent flow from leaving the end-wall boundary layer was calculated from Eq. (A21) for the aforementioned flow conditions and is presented in Fig. 19. (The friction ratio, $C_{ft} / C_{ft,6}$, for the constant-density case varies as $1 / R^4$.) The effect of the variable density is not large; the increase in required $C_{ft}$ is less than 20% for all radii for $h_d = 0.1 V_\phi$. Note in particular that the effect is most pronounced where $C_{ft,6}$ is small near $R = 1$. Near the center of the vortex where the actual skin-friction coefficient is very large, secondary-flow density gradients have almost no effect.

The variation of boundary layer thickness with radius was calculated using Eq. (A30) for the primary and secondary-flow conditions shown on Figs. 18 and 19. These results are presented in Fig. 20. When no mass transfer occurs ($h_d = 0$) so that the secondary flow has a constant density, the effect of a variable primary-flow density is to thin the boundary layer at all radii. As the mass-transfer coefficient increases, the boundary layer thickness becomes larger at all radii and, for the largest mass-transfer coefficient studied, the boundary layer near $r_6$ was thicker than that for the constant-density case (also shown in Fig. 20).

The dimensionless time constant for the flow with distributed friction is

$$\tau_{SF} = t_{SF} / (r_6^2 / \nu) = \frac{\int_0^1 \bar{\rho}_{pH} R \, dR}{S_6 \bar{\rho}_{SH,10}} \tag{8}$$

where $\bar{\rho}_{pH}$ and $\bar{\rho}_{SH}$ are the dimensionless heavy-gas densities in the primary and secondary-flow regions, respectively. The variation of $\tau_{SF}$ with G for $h_d = G_1 V_\phi$ and $h_d = G_2 V_{\phi,6}$ is shown in Fig. 21. The effect of increasing the diffusion velocities is to decrease the time constant. The lower limit for the time constant, also shown on the figure, occurs when the primary-flow and secondary-flow densities are equal.

Distributed Suction

The variation of secondary-flow density with radius ratio is presented in Fig. 22 for $h_d = 0.001 V_\phi$, $0.01 V_\phi$, $0.1 V_\phi$, and $0.01 V_{\phi,6}$ values of $\xi / K_7 = 1.25$ and $K_7 / C_{ft,0} = 160$ were assumed in the calculations for this figure. The shapes of the $\bar{\rho}_s$ profiles are similar to those obtained with secondary-flow control by distributed-friction end walls near $R = 1$. However, at smaller radii, $R < 0.8$, the values of $\bar{\rho}_s$ are larger with distributed suction and a given mass-transfer coefficient, since less flow remains in the end-wall boundary layer to dilute the incoming heavy gas.

The variation of dimensionless secondary flow with radius ratio is presented in Fig. 23. The profiles indicate that additional fluid must be removed from the boundary layer when diffusion occurs to provide the increase skin friction required for removal of the angular momentum gained by the diffusion of the heavier fluid with its higher angular momentum into the secondary flow.

The effect of axial mass transfer from a variable-density primary flow on the variation of boundary layer thickness with radius is shown in Fig. 24. The variation of $\delta$ with radius for the constant-density case is also shown for comparison. The results are similar to those shown for the example with distributed friction in that the increased pressure gradient, which exists when the primary flow has a variable density, forces the boundary layer for a constant-density secondary flow ($h_d = 0$) to thin more than when both the primary and secondary flows have constant density. The boundary layers for increased values of $h_d$ are thicker than for smaller values of $h_d$ even though less flow is in the end-wall boundary layers.

A secondary-flow dimensionless time constant, $\tau_{SF}$, is defined analogous to that for the distributed-friction case.

$$\tau_{SF} = \frac{\int_0^1 \bar{\rho}_{pH} R \, dR}{S_6 \int_0^1 \bar{\rho}_{sH} \left( \frac{d\bar{Q}_s}{dR} \right) dR} \tag{9}$$

The variation of the dimensionless secondary-flow time constant with the axial-mass-transfer parameter is presented in Fig. 25. The mass-transfer coefficient which is independent of radius, $h_d = G_2 V_{\phi,6}$, yields a lower time constant than the variable mass-transfer coefficient, $h_d = G_1 V_\phi$, when $G_1 = G_2 = 10^{-3}$. However, where $G_1 = G_2 = 10^{-1}$ the situation is reversed since the flow characterized by $h_d = G_2 V_{\phi,6}$ has much less secondary flow at small radii than the flow characterized by $h_d = G_1 V_\phi$. The time constant, which would occur if $\bar{\rho}_s$ were equal to $\bar{\rho}_{p,10}$ at all radii, is shown for comparison.

REFERENCES

1. Mack, Leslie M.: The Laminar Boundary Layer on a Disk of Finite Radius in a Rotating Flow. Part I: Numerical Integration of the Momentum-Integral Equations and Application of the Results to the Flow in a Vortex Chamber. JPL Technical Report No. 32-224. May 20, 1962.

2. King, W. S.: Momentum-Integral Solutions for the Laminar Boundary Layer on a Finite Disk in a Rotating Flow. Aerospace Corp. Report ATN-63(9227)-3. June 18, 1963.

3. Anderson, Olof: Theoretical Solutions for the Secondary Flow in the End Wall of a Vortex Tube. UAC Research Laboratories Report R-2494-1. November 1961.

4. Anderson, O. L.: Theoretical Effect of Mach Number and Temperature Gradient on Primary and Secondary Flow in a Jet-Driven Vortex. Air Force Systems Command Report RTD-TDR-63-1098, Prepared by UAC Research Laboratories. November 1963.

5. Owen, F. S., R. W. Hale, B. V. Johnson, and A. Travers: Experimental Investigation of Characteristics of Confined Jet-Driven Vortex Flows. UAC Research Laboratories Report No. R-2494-2, November 1961. Confidential.

6. Kendall, James M.: Experimental Study of a Compressible Viscous Vortex. JPL Technical Report No. 32-290. June 5, 1962.

7. Johnson, B. V., A. Travers, and R. W. Hale: Measurements of Flow Patterns in a Jet-Driven Vortex. Air Force Systems Command Report RTD-TDR-63-1094, Prepared by UAC Research Laboratories, November 1963. Confidential.

8. Schlichting, Hermann: Boundary Layer Theory. 4th Ed. McGraw-Hill. 1960.

9. Eckert, E. R. G. and R. Drake: Heat and Mass Transfer. Second Edition, McGraw-Hill, 1959.

## LIST OF SYMBOLS

| | |
|---|---|
| $C_{fr}$ | Radial-skin-friction coefficient, dimensionless |
| $C_{ft}$ | Tangential-skin-friction coefficient, dimensionless |
| $C_{ft,o}$ | Tangential-skin-friction coefficient on end wall without secondary-flow control (assumed constant for a given flow condition), dimensionless |
| $f_1(\eta)$ | Tangential velocity function, $U_\phi / V_\phi$ |
| $f_2(\eta)$ | Radial velocity function, $U_r / \bar{U}_r V_{\phi,6}$ |
| $G_1$ | Axial-mass-transfer parameter, $h_d / V_\phi$, dimensionless |
| $G_2$ | Axial-mass-transfer parameter, $h_d / V_{\phi,6}$, dimensionless |
| $h_d$ | Axial-mass-transfer coefficient, ft/sec |
| $J$ | Secondary-flow parameter, $Re_{t,6} / (2 S_6 K_7)$, dimensionless |
| $K_i$ | Integration constants for momentum-integral analysis (see Table II), dimensionless |
| $L$ | Length of vortex tube, ft |
| $\dot{m}$ | Mass transfer rate due to axial diffusion (see Eq. (A3)), $lb/ft^2 sec$ |
| $n_\Gamma$ | Exponent for primary-flow circulation function, $\bar{\Gamma} = V_\phi r / (V_{\phi,6} r_6) = R^{n_\Gamma}$ |
| $Q_s$ | Secondary volume flow rate in one end-wall boundary layer (flow outward is positive), $ft^3/sec$ |
| $\bar{Q}_s$ | $\frac{\text{Secondary volume flow rate in one end-wall boundary layer}}{\text{Secondary volume flow rate in one end-wall boundary layer at } r_6}$ |
| $r$ | Radius, ft |
| $R$ | Dimensionless radius, $r/r_6$ or $r/r_1$ |
| $Re_{rp}$ | Primary-flow radial Reynolds number $-V_r r / \nu$ |

| | |
|---|---|
| $Re_{t,1}$ | Tangential Reynolds number based on conditions at radius $r_1$ , $V_{\phi,1} r_1 / \nu$ |
| $Re_{t,6}$ | Tangential Reynolds number based on conditions at radius $r_6$ , $V_{\phi,6} r_6 / \nu$ |
| $S_6$ | Dimensionless secondary flow, $-Q_{s,6} / (2\pi\nu r_6)$ |
| $\bar{S}$ | $\frac{\text{Secondary-flow rate in one end-wall boundary layer}}{\text{Reference secondary-flow rate in one end-wall boundary layer}}$ |
| $t_{SF}$ | Secondary-flow time constant (see Eqs. (8) and (9)), sec |
| $U_r$, $U_\phi$, $U_z$ | Radial, tangential and axial velocities within the end-wall boundary layer (secondary-flow region), ft/sec |
| $U_{r,MAX}$ | Maximum radial velocity in boundary layer (see Eq. (A28)), ft/sec |
| $\bar{U}_r$ | Average radial velocity in end-wall boundary layer (see Eq. (A15)) (positive outward), dimensionless |
| $U_{z,w}$ | Wall suction velocity (always positive), ft/sec |
| $U_{z,\delta}$ | Axial velocity at distance $\delta$ from the end wall, ft/sec |
| $V_r$, $V_\phi$, $V_z$ | Radial, tangential, and axial velocities outside of end-wall boundary layer, ft/sec |
| $z$ | Axial distance, ft |
| $\Gamma$ | Circulation, $V_\phi r$ , $ft^2/sec$ |
| $\bar{\Gamma}$ | Dimensionless circulation, $V_\phi r / (V_{\phi,6} r_6)$ or $V_\phi r / (V_{\phi,1} r_1)$ |
| $\delta$ | Boundary layer thickness, ft, in. |
| $\eta$ | Axial boundary layer parameter, $z/\delta$ |
| $\nu$ | Kinematic viscosity, $ft^2/sec$ |
| $\xi$ | Suction parameter for asymptotic skin-friction coefficient (Eq. (A23)), dimensionless |
| $\rho_p$ | Primary-flow density, $lb/ft^3$ |
| $\bar{\rho}_p$ | Dimensionless primary-flow density ratio, $\rho_p / \rho_{p,6}$ |
| $\bar{\rho}_{pH}$ | Dimensionless heavy-gas density in primary-flow region, $\rho_{pH} / \rho_{p,6}$ |

| | |
|---|---|
| $\rho_s$ | Average secondary-flow density (see Eq. (A1)), $lb/ft^3$ |
| $\bar{\rho}_s$ | Dimensionless secondary-flow density, $\rho_s/\rho_{p,6}$ |
| $\bar{\rho}_{SH}$ | Dimensionless heavy-gas density in boundary layer, $\rho_{SH}/\rho_{p,6}$ |
| $\tau_{SF}$ | Dimensionless secondary-flow time constant (see Eqs. (8) and (9)) |
| $\phi$ | Azimuthal location, degrees, radians |
| $\theta$ | Boundary layer parameter, $r\delta$ , $ft^2$ |
| $\Theta$ | Dimensionless boundary layer parameter, $r\delta/r_6\delta_6$ |

Subscripts

| | |
|---|---|
| 1 | Outside radius of tube |
| 6 | Largest radius where primary radial flow is constant |
| 10 | Exit radius |

# APPENDIX

## DERIVATION OF EQUATIONS FOR SECONDARY-FLOW CONTROL

The tangential-momentum, radial-momentum and mass-continuity equations are used to analyze the flow model shown in Figs. 1, 2 and 26 for the conditions where no fluid is convected between the primary and secondary-flow regions. Using the assumptions enumerated in Table I, the tangential-momentum boundary layer integral equation is used to determine the skin friction (dissipation produced by wall protrusions) or wall suction distributions which satisfy the boundary condition of zero axial velocity between the primary and secondary flows. The radial-momentum equation is used to determine the effect of the increased wall friction or wall suction on the variation of boundary layer thickness with radius. For flows with variable density, the boundary condition of zero axial velocity is still maintained; however, mass transfer by diffusion may occur.

### Mass-Transfer Equation

Consider the flow model shown in Figs. 2 and 26: The density of the primary flow is taken to be a function of the radius and independent of axial distance outside the end-wall boundary layer. The secondary-flow density is assumed continuous through the boundary layer and at the axial station of the edge of the boundary layer, $\delta$. Since an integral boundary layer analysis is to be employed, an average secondary-flow density, defined as

$$\rho_s = \int_0^\delta \rho U_r \, dz \Big/ \int_0^\delta U_r \, dz \tag{A1}$$

will be used for computational purposes.

An axial-mass-transfer coefficient is defined analogous to the turbulent-heat-transfer coefficient (Ref. 9). The diffusive mass transfer between the primary and secondary flows for a two-component mixture is given in terms of the primary-flow density and the average secondary-flow density as

$$\dot{m} = \dot{m}_a + \dot{m}_b = h_{d,a} \left( \rho_{p,a} - \rho_{s,a} \right) + h_{d,b} \left( \rho_{p,b} - \rho_{s,b} \right) \tag{A2}$$

where the subscripts a and b refer to the species in a two-component gas. For the usual condition where $h_{d,a} = h_{d,b}$ the mass-transfer rate becomes a function only of the primary and secondary-flow densities. (Note that $h_d$ has the dimensions of velocity.)

$$\dot{m} = h_d \left( \rho_p - \rho_s \right) \tag{A3}$$

From the flow model (Fig. 26), the mass transfer into the boundary layer through an element of radius $r$ and thickness $dr$ is

$$\dot{m}\, 2\pi r\, dr = h_d \left( \rho_p - \rho_s \right) 2\pi r\, dr \tag{A4}$$

A mass balance on the unit volume shown yields

$$\rho_s Q_s + h_d \left( \rho_p - \rho_s \right) 2\pi r\, dr = \rho_s Q_s + \frac{d}{dr} \left( \rho_s Q_s \right) dr + 2\pi \rho_s \left| U_{z,w} \right| r\, dr \tag{A5}$$

For a variable secondary flow due to wall suction

$$\frac{dQ_s}{dr} = -2\pi r \left| U_{z,w} \right| \tag{A6}$$

Combining Eq. (A5) with (A6) gives

$$\frac{h_d \left( \rho_p - \rho_s \right) 2\pi r}{Q_s} = \frac{d\rho_s}{dr} \tag{A7}$$

Equation (A7) can be integrated to obtain the variation of $\rho_s$ with radius for given radial distributions of $Q_s$, $\rho_p$ and $h_d$. To facilitate the calculation procedure, Eq. (A7) is made nondimensional with respect to radius $r_\delta$ (the outer radius which satisfies the boundary condition $U_{z,\delta} = 0$), $Q_{s,\delta}$ and $\rho_{p,\delta}$. In addition, the axial-mass-transfer coefficient $h_d$ will be assumed to be a function only of the primary-flow tangential velocity in the form

$$h_d = G_1 V_\phi \tag{A8}$$

or

$$h_d = G_2 V_{\phi,6} \tag{A9}$$

The analogy between heat transfer and mass transfer on a flat plate presented in Ref. 9 indicates that the ratio of $h_d/V$ is only a weak function of Reynolds, Schmidt and Prandtl numbers. Typical values of $h_d/V$ are between 0.006 and 0.003 for a Schmidt number of 1.

In nondimensional form Eq. (A7) becomes

$$\frac{d\bar{\rho}_s}{dR} = \left(\frac{2\pi\nu r_6}{Q_{s,6}}\right)\left(\frac{V_{\phi,6} r_6}{\nu}\right) G_1 \bar{\Gamma} \frac{(\bar{\rho}_p - \bar{\rho}_s)}{\bar{Q}_s} = \frac{Re_{t,6}}{S_6} G_1 \bar{\Gamma} \frac{(\bar{\rho}_p - \bar{\rho}_s)}{\bar{Q}_s} \tag{A10}$$

for an axial-mass-transfer coefficient defined by Eq. (A8) and

$$\frac{d\bar{\rho}_s}{dR} = -\frac{Re_{t,6}}{S_6} \frac{G_2 R}{\bar{Q}_s} (\bar{\rho}_p - \bar{\rho}_s) \tag{A11}$$

for an axial-mass-transfer coefficient defined by Eq. (A9). $Re_{t,6}$ and $S_6$ are defined as the tangential Reynolds number and dimensionless secondary-flow rate at $r_6$, respectively.

## Tangential-Momentum Equation

Consider the following integral form of the boundary layer tangential-momentum equation (analogous to that presented in Ref. 1) in cylindrical coordinates.

$$\frac{d}{dr} \int_0^{\delta} (2\pi r \rho_s U_r)(r U_\phi)\, dz = +(V_\phi r)\, 2\pi r h_d (\rho_p - \rho_s) - \pi C_{ft} \rho_s V_\phi^2 r^2 \tag{A12}$$

where $C_{ft} \rho_s \frac{V_\phi^2}{2}$ is the tangential shear stress at the wall. In deriving Eq. (A12) it has been assumed that there is no convection between the primary and secondary-flow regions (i.e., $U_{z,\delta} = 0$) but that diffusive mass transfer can occur between these two regions in accordance with Eq. (A3). The first term on the right side of Eq. (A12) represents the rate at which angular momentum is transferred between the end-wall boundary layer and the primary flow by the axial mass transfer. The second term represents the rate at which angular momentum is decreased by end-wall skin friction. The left-side term represents the radial gradient of the angular momentum flux of the secondary flow.

In the manner of Ref. 3, the following quantities are defined:

$$\eta = z / \delta \tag{A13}$$

$$f_1(\eta) = U_\phi / V_\phi \tag{A14}$$

$$f_2(\eta) = U_r / \bar{U}_r V_{\phi,6} \tag{A15}$$

where $\bar{U}_r$ is the ratio of the average radial velocity in the end-wall boundary layer to the primary-flow tangential velocity at $r_6$. By this definition

$$\int_0^1 f_2(\eta)\, d\eta = 1 \tag{A16}$$

and

$$Q_s = +2\pi r \int_0^\delta U_r\, dz = 2\pi r \delta \bar{U}_r V_{\phi,6} \tag{A17}$$

By use of Eqs. (A7) and (A13) through (A17), Eq. (A12) can be rewritten to give

$$\frac{d}{dr}\left\{Q_s \rho_s \Gamma K_7\right\} = \Gamma Q_s \frac{d\rho_s}{dr} - \rho_s \pi C_{ft} \Gamma^2 \tag{A18}$$

where

$$K_7 = \int_0^1 f_1(\eta)\, f_2(\eta)\, d\eta \tag{A19}$$

$K_7$ is assumed constant for a given set of flow conditions (see Table II for value employed in analysis). To prevent flow from leaving the end-wall boundary layer, Eq. (A18) must be satisfied for all radii less than $r_6$.

Distributed Friction

For the desired distributed friction, $Q_s$ is constant and equal to $Q_{s,6}$ so Eq. (A18) can be rewritten to give

$$\frac{d\rho_s}{dr}\,\Gamma(K_7-1)+K_7\rho_s\frac{d\Gamma}{dr}=-\rho_s\frac{\pi}{Q_{s,6}}\,\Gamma^2 C_{ft} \tag{A20}$$

To facilitate the calculation procedure, Eq. (A20) is made nondimensional with respect to $r_6$, $\Gamma_6$ and $\rho_{p,6}$ and rearranged to obtain $C_{ft}$.

$$C_{ft}=\frac{1}{J}\left[\frac{1}{\bar{\Gamma}^2}\frac{d\bar{\Gamma}}{dR}+\frac{1}{\bar{\Gamma}\bar{\rho}_s}\frac{d\bar{\rho}_s}{dR}\left(1-\frac{1}{K_7}\right)\right] \tag{A21}$$

where

$$J=\frac{Re_{t,6}}{2S_6K_7}=-\left(\frac{V_{\phi,6}\,r_6}{\nu}\right)\left(\frac{\pi\nu r_6}{Q_{s,6}}\right)\frac{1}{K_7} \tag{A22}$$

The required variation of $C_{ft}$ with radius which satisfies the condition that $U_{z,\delta}=0$ can be obtained directly from Eq. (A21) for any known primary-flow circulation distribution and secondary-flow density distribution obtained from the solution at Eq. (A10) or Eq. (A11).

Distributed Suction

For the condition where there is the increased friction due to wall suction, the tangential-skin-friction coefficient will be given as

$$C_{ft}=C_{ft,0}+\xi\,2U_{z,w}/V_\phi \tag{A23}$$

where $C_{ft,0}$ is the skin-friction coefficient which would occur on a smooth wall and is constant for a given set of flow conditions. Recall that $U_{z,\delta}=0$ for $r\le r_6$, and thus

$$\frac{dQ_s}{dr}=-2\pi r U_{z,w} \tag{A24}$$

By making use of this fact, Eq. (A18) can be rewritten for the distributed-suction condition as

$$\frac{d}{dr}\left\{Q_s \rho_s \Gamma K_7\right\} - \Gamma Q_s \frac{d\rho_s}{dr} = - C_{ft,o} \rho_s \Gamma^2 \pi + \xi \rho_s \Gamma \frac{dQ_s}{dr} \qquad \text{(A25)}$$

By combining terms and again making nondimensional with respect to radius $r_6$, $Q_{s,6}$, and $\rho_{p,6}$, Eq. (A25) becomes

$$\frac{d\bar{Q}_s}{dR} = \left[\frac{K_7}{\xi - K_7}\right]\left\{\frac{\bar{Q}_s}{\bar{\rho}_s}\frac{d\bar{\rho}_s}{dR}\left(\frac{1-K_7}{K_7}\right) + \frac{\bar{Q}_s}{\bar{\Gamma}}\frac{d\bar{\Gamma}}{dR} - C_{ft,o} J \bar{\Gamma}\right\} \qquad \text{(A26)}$$

where J is defined by Eq. (A22). The dimensionless end-wall suction rate may be obtained by simultaneous solution of either Eqs. (A10) or (A11), as appropriate, and Eq. (A26). The variation of the dimensionless secondary flow, $\bar{Q}_s$, with radius ratio, R, can be obtained by integration of Eq. (A26).

## Radial-Momentum Equation

Consider the following form of the radial-momentum integral equation (analogous to that presented in Ref. 1) in cylindrical coordinates for a flow with the primary and secondary-flow densities outlined previously.

$$\frac{d}{dr}\int_0^\delta (2\pi \rho_s r U_r) U_r \, dz + 2\pi \int_0^\delta \left(\rho_p V_\phi^2 - \rho_s U_\phi^2\right) dz = r\pi C_{fr} \rho_s U_{r,MAX}^2 \qquad \text{(A27)}$$

where $\frac{1}{2}\rho_s C_{fr} U_{r,MAX}^2$ is the radial shear stress at the wall. $U_{r,MAX}$ is the maximum radial velocity in the end-wall boundary layer and is related to the radial mass flow by

$$\frac{U_{r,MAX}}{\bar{U}_r V_{\phi,6}} = f_{2,MAX} \qquad \text{(see Table II)} \qquad \text{(A28)}$$

For this analysis the radial flow in the end-wall boundary layer is toward the origin of the coordinate system. The sign convention given in Eq. (A27) yields the proper terms for both the distributed-friction and distributed-suction boundary layer thickness calculations.

Distributed Friction

Assume that the radial-skin-friction coefficient is equal to the tangential-skin-friction coefficient required to satisfy the condition $U_{z,\delta} = 0$ (see Eq. (A21). Equation (A27) may be combined with Eqs. (A13) to (A17) and Eq. (A28) to give

$$\frac{d}{dr}\left\{\frac{Q_s^2 \rho_s}{4\pi^2 r\delta}\int_0^1 f_2^2(\eta)\,d\eta\right\} + \delta\rho_p V_\phi^2 - \delta\rho_s V_\phi^2 \int_0^1 f_1^2\,d\eta =$$

$$\rho_s \frac{Q_s^2}{8\pi^2} \frac{f_{2,MAX}^2}{\delta^2 r} C_{ft} \tag{A29}$$

By using the integral constants $K_4$ and $K_8$ defined in Table II, letting $\theta = r\delta$ and again making the equation nondimensional with respect to radius $r_6$, $Q_{s,6}$, $\rho_{p,6}$, and $\delta_6$, Eq. (A29) may be rewritten as a first order differential equation in $\Theta = \theta/\theta_6$

$$\frac{d\Theta}{dR} = \frac{\Delta_1 \Theta^3 \bar{\Gamma}^2}{\bar{\rho}_s R^3}\left[\frac{\bar{\rho}_p - \bar{\rho}_s}{K_8} + \bar{\rho}_s\right] - \Delta_2 R \frac{C_{ft}}{C_{ft,6}} + \frac{\Theta}{\bar{\rho}_s}\frac{d\bar{\rho}_s}{dR} \tag{A30}$$

where

$$\Delta_1 = \frac{Re_{t,6}^2}{S_6^2}\left(\frac{\delta_6}{r_6}\right)^2 \frac{K_8}{K_4} \tag{A31}$$

and

$$\Delta_2 = \frac{C_{ft,6} f_{2,MAX}^2}{2K_4}\left(\frac{r_6}{\delta_6}\right) \tag{A32}$$

The variation of $\Theta$ with $R$ and hence $\delta$ with $r$ can be obtained by integrating Eq. (A30) in conjunction with the solution of Eqs. (A10) or (A11).

Distributed Suction

Assume a radial-skin-friction coefficient analogous to the tangential-skin-friction coefficient

$$C_{fr} = C_{ft,0} + \xi 2 U_{z,w} / U_{r,MAX} \tag{A33}$$

By combining Eqs. (A27) and (A33) with Eqs. (A13) to (A17), the following form of the radial-momentum equation is obtained.

$$\frac{d}{dR}\left\{\frac{Q_s^2 \rho_s}{4\pi r \delta}\int_0^1 f_2(\eta)^2 d\eta\right\} + \rho_p V_\phi^2 \delta - \rho_s V_\phi^2 \delta \int_0^1 f_1(\eta)^2 d\eta = \tag{A34}$$

$$\frac{\rho_s C_{ft,0} Q_s^2 f_{2,MAX}^2}{8\pi^2 r \delta^2} + \frac{\rho_s \xi Q_s f_{2,MAX}}{4\pi^2 r \delta}\frac{dQ_s}{dr}$$

By using the integral constants $K_4$ and $K_8$ defined in Table II letting $\theta = r\delta$ and making the equation nondimensional with respect to radius $r_6$, $Q_{s,6}$, $\rho_{p,6}$, and $\delta_6$, Eq. (A34) can be rewritten as a first order differential equation for $\Theta = \theta/\theta_6$.

$$\frac{d\Theta}{dR} = \frac{\Delta_1 \bar{\Gamma}^2 \Theta^3}{\bar{Q}_s^2 R^3}\left[\frac{\bar{\rho}_p - \bar{\rho}_s}{K_8} + \bar{\rho}_s\right] - \Delta_2 R + \frac{\Theta}{\bar{\rho}_s}\frac{d\bar{\rho}_s}{dR} + \Delta_3 \frac{\Theta}{\bar{Q}_s}\frac{d\bar{Q}_s}{dR} \tag{A35}$$

where $\Delta_1$ and $\Delta_2$ are given by Eqs. (A31) and (A32) and

$$\Delta_3 = 2 - (f_{2,MAX}\,\xi) / K_4 \tag{A36}$$

The variation of $\Theta$ with $R$ and hence $\delta$ with $r$ can be obtained by integrating Eq. (A35), beginning at radius $r_6$.

TABLE I

ASSUMPTIONS FOR ANALYSIS OF SECONDARY-FLOW-CONTROL METHODS

1. The flow is steady.

2. The pressure, density, and tangential velocity in the primary flow outside the end-wall boundary layer are functions only of radius.

3. Velocity profiles are similar for a given flow condition so that the integration constants given in Table II are independent of radius.

4. The skin-friction coefficient is independent of boundary layer thickness.

5. The tangential-momentum equation is decoupled from the radial-momentum equation since $C_{ft}$ is not a function of the boundary layer thickness $\delta$.

6. Radial and tangential boundary layer thicknesses are identical.

7. The radial-skin-friction coefficient is equal to the tangential-skin-friction coefficient.

8. The axial-mass-transfer coefficient is given by $h_d = G_1 V_\phi$ or by $h_d = G_2 V_{\phi,\delta}$ and is not a function of boundary layer thickness or boundary layer Reynolds number (see discussion in Appendix).

9. When end-wall suction is employed to increase skin friction the skin-friction coefficient is $C_{ft} = C_{ft,0} + \xi 2 U_{z,w} / V_\phi$.

10. The skin-friction coefficient $C_{ft,0}$ is constant with radius.

11. The required variation of friction coefficient for the distributed-friction secondary-flow-control method can be obtained by protrusions from the end wall into the boundary layer.

TABLE II

TABLE OF BOUNDARY LAYER INTEGRALS AND ASSUMED VALUES USED IN ANALYSIS

| CONSTANT | DEFINITION | FUNCTIONAL RELATION | ASSUMED IN ANALYSIS OF REFS. 3 AND 4 | MEASURED IN EXPERIMENT OF REF. 5 | ASSUMED FOR THIS ANALYSIS |
|---|---|---|---|---|---|
| $K_4$ | $\frac{1}{\delta}\int_0^{\delta}\left(\frac{U_r}{V_{\phi,6}\,\overline{U}_r}\right)^2 dz$ | $\int_0^1 f_2^2\, d\eta$ | 1.678 | 1.356 | 1.4 |
| $K_7$ | $\frac{1}{\delta}\int_0^{\delta}\left(\frac{U_r}{V_{\phi,6}\,\overline{U}_r}\right)\left(\frac{U_\phi}{V_\phi}\right) dz$ | $\int_0^1 f_1 f_2\, d\eta$ | 0.795 | 0.801 | 0.8 |
| $K_8$ | $\frac{1}{\delta}\int_0^{\delta}\left[1-\left(\frac{U_\phi}{V_\phi}\right)^2\right] dz$ | $\int_0^1 (1-f_1^2)\, d\eta$ | 0.222 | - | 0.2 |
| $f_{2,MAX}$ | $\frac{U_{r,\,MAX}}{V_{\phi,6}\,\overline{U}_r}$ | | 2.42 | 2.05 | 2.0 |

UNCLASSIFIED
CONFIDENTIAL

CONFIDENTIAL
UNCLASSIFIED

TABLE III

PARAMETERS EMPLOYED IN DESCRIBING VORTEX SECONDARY-FLOW-CONTROL SYSTEMS

| Parameter | Comments |
|---|---|
| $C_{ft,o}$ | Tangential-skin-friction coefficient on plain end wall without artificially increased friction and without suction. |
| $C_{ft}$ | Tangential-skin-friction coefficient. For suction end wall, $C_{ft} = C_{ft,o} + \xi(2U_{z,w}/V_\phi)$ |
| $C_{ft,s}$ | Value of local friction coefficient at outermost radius for which flow in end-wall boundary layer does not vary with radius (i.e., $dQ_s/dr = 0$ ). This friction coefficient may either be one which is naturally occurring or one which is artificially increased. |
| $h_d$ | Axial-mass-transfer coefficient governing rate at which heavy gas in primary flow diffuses into secondary flow. Assumed equal to zero except in Figs. 18 through 25. |
| $K_7$ | $\frac{\text{Average angular momentum flux in secondary flow}}{\text{(Angular momentum flux in secondary flow if all fluid had primary-flow tangential velocity)}}$<br><br>$K_7$ assumed equal to 0.8 in all calculations. |
| $\xi$ | Ratio of the rate of secondary-flow angular momentum decrease by suction to the angular momentum flux which would occur by an equivalent flow withdrawal rate from the primary-flow region. |
| $\xi/K_7$ | Parameter relating decrease in angular momentum within boundary layer due to suction to the average angular momentum of secondary flow in end-wall boundary layer. $\xi/K_7$ must be greater than unity if end-wall suction is to result in a decrease in the average angular momentum in the boundary layer. |

UNCLASSIFIED

# GEOMETRY AND FLOW REGIONS FOR CONFINED VORTEX FLOW

FLUID PASSES FROM PRIMARY FLOW TO SECONDARY FLOW FOR $r > r_6$

FLUID PASSES FROM SECONDARY FLOW TO PRIMARY FLOW FOR $r < r_6$ IF NO SECONDARY-FLOW CONTROL IS EMPLOYED.
OBJECT OF SECONDARY-FLOW CONTROL IS TO MAINTAIN CONSTANT PRIMARY FLOW FOR $r < r_6$ (i.e., IN PRIMARY-FLOW REGION 2)

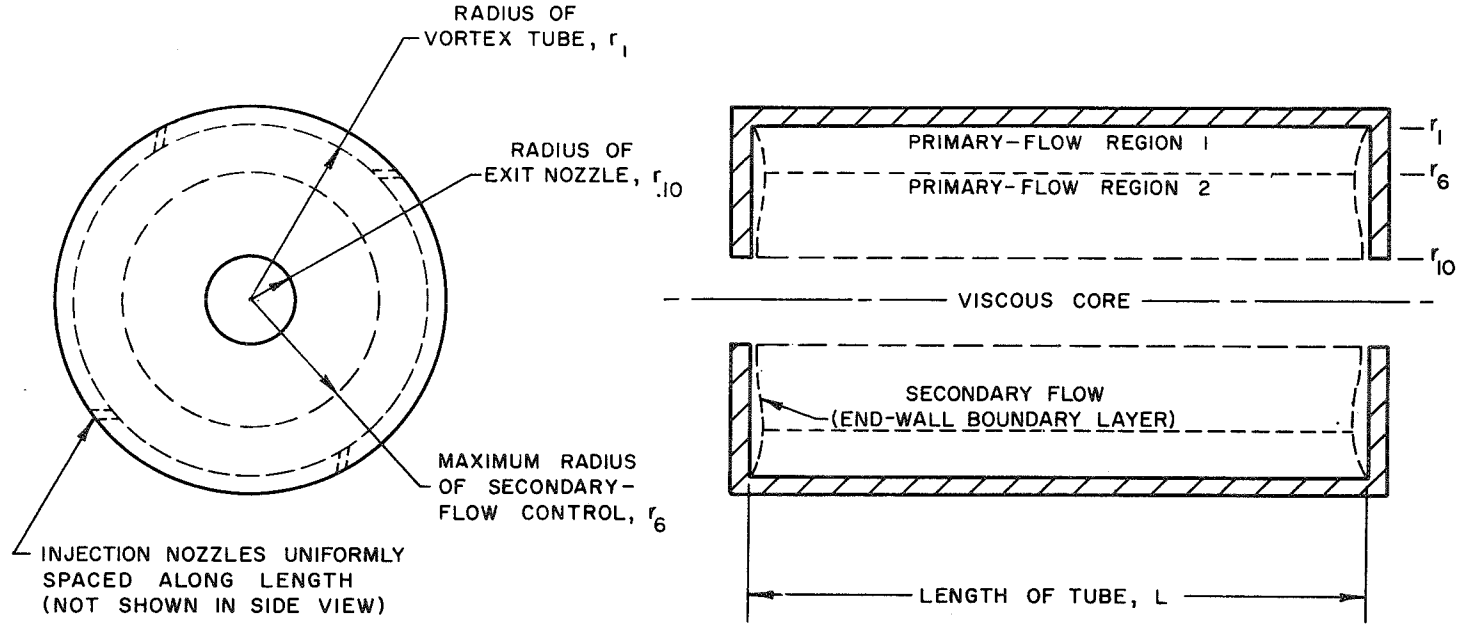


Figure 1

UNCLASSIFIED

Figure 2

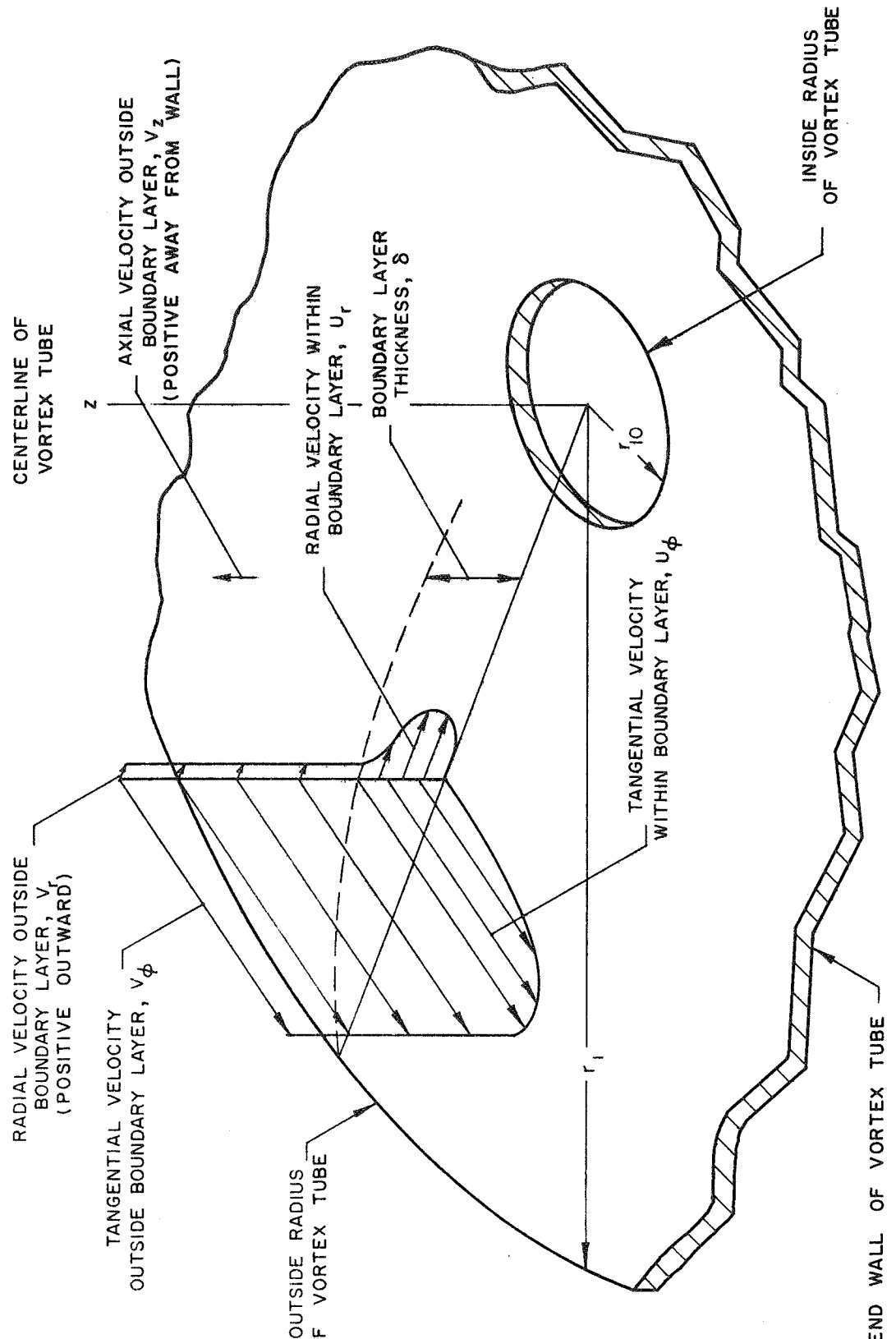
VELOCITIES CONSIDERED IN ANALYSIS
NOTE: $V_{\phi,1}$ AND $V_{r,1}$ ARE VALUES OF $V_\phi$ AND $V_r$ AT $r = r_1$
CENTERLINE OF VORTEX TUBE
z
AXIAL VELOCITY OUTSIDE BOUNDARY LAYER, $V_z$ (POSITIVE AWAY FROM WALL)
RADIAL VELOCITY WITHIN BOUNDARY LAYER, $U_r$
BOUNDARY LAYER THICKNESS, $\delta$
INSIDE RADIUS OF VORTEX TUBE
$r_{10}$
RADIAL VELOCITY OUTSIDE BOUNDARY LAYER, $V_r$ (POSITIVE OUTWARD)
TANGENTIAL VELOCITY OUTSIDE BOUNDARY LAYER, $V_\phi$
TANGENTIAL VELOCITY WITHIN BOUNDARY LAYER, $U_\phi$
OUTSIDE RADIUS OF VORTEX TUBE
$r_1$
END WALL OF VORTEX TUBE

# TANGENTIAL VELOCITY AND CIRCULATION DISTRIBUTIONS IN VORTEX

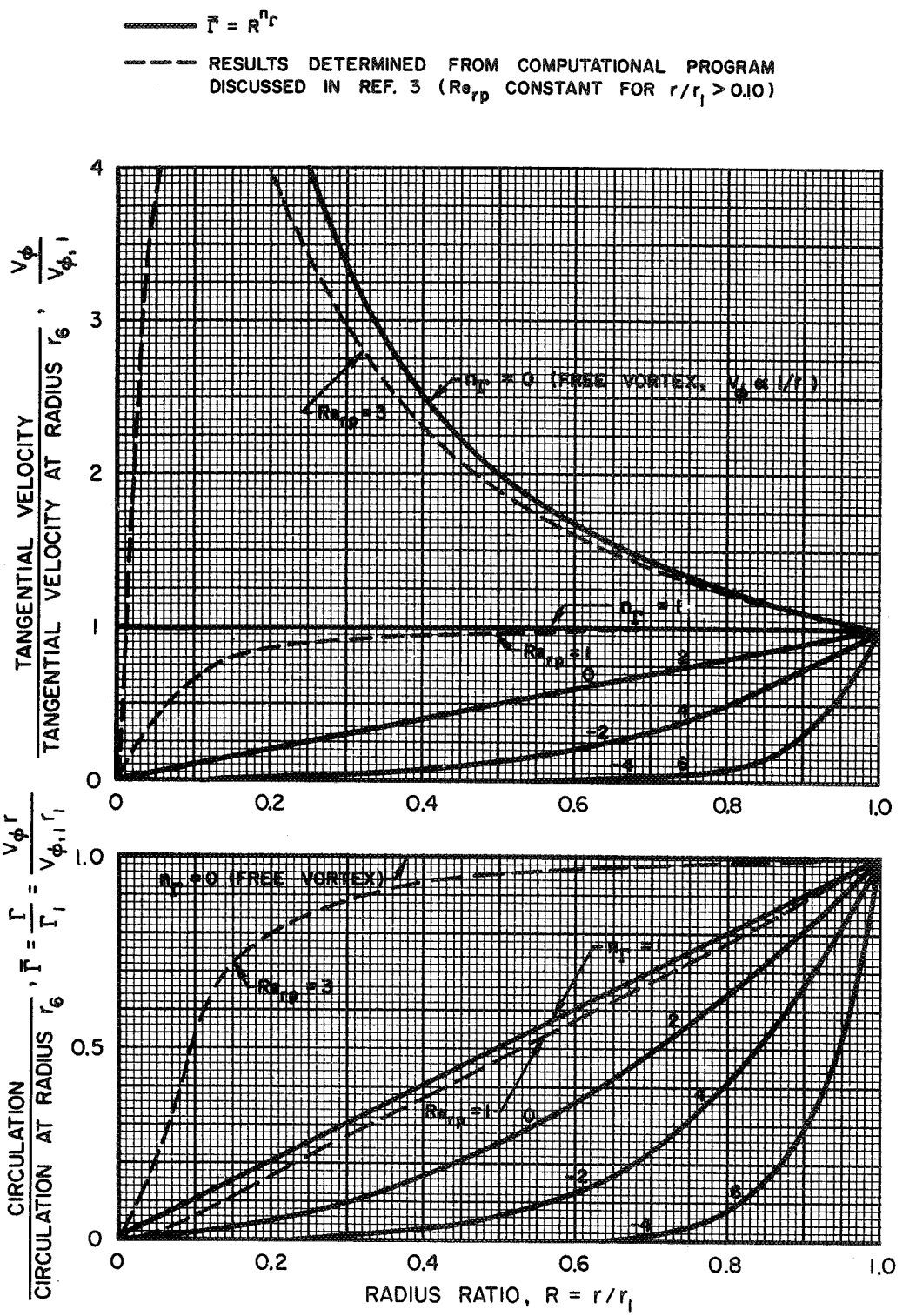
$\bar{\Gamma} = R^{n_r}$
RESULTS DETERMINED FROM COMPUTATIONAL PROGRAM DISCUSSED IN REF. 3 ($Re_{rp}$ CONSTANT FOR $r/r_1 > 0.10$)
TANGENTIAL VELOCITY / TANGENTIAL VELOCITY AT RADIUS $r_6$, $\frac{V_\phi}{V_{\phi,1}}$
$n_r = 0$ (FREE VORTEX, $V_\phi \propto 1/r$)
$Re_{rp} = 3$
$n_r = 1$
$Re_{rp} = 1$
0
2
3
-2
-4
6
CIRCULATION / CIRCULATION AT RADIUS $r_6$, $\bar{\Gamma} = \frac{\Gamma}{\Gamma_1} = \frac{V_\phi r}{V_{\phi,1} r_1}$
$n_r = 0$ (FREE VORTEX)
RADIUS RATIO, $R = r/r_1$

# VARIATION OF DIMENSIONLESS SECONDARY FLOW WITH RADIUS FOR SEVERAL PRIMARY-FLOW CIRCULATION DISTRIBUTIONS

RESULTS DETERMINED FROM COMPUTATIONAL PROGRAM DISCUSSED IN REF. 4

SEE FIG. 3 FOR CIRCULATION DISTRIBUTIONS

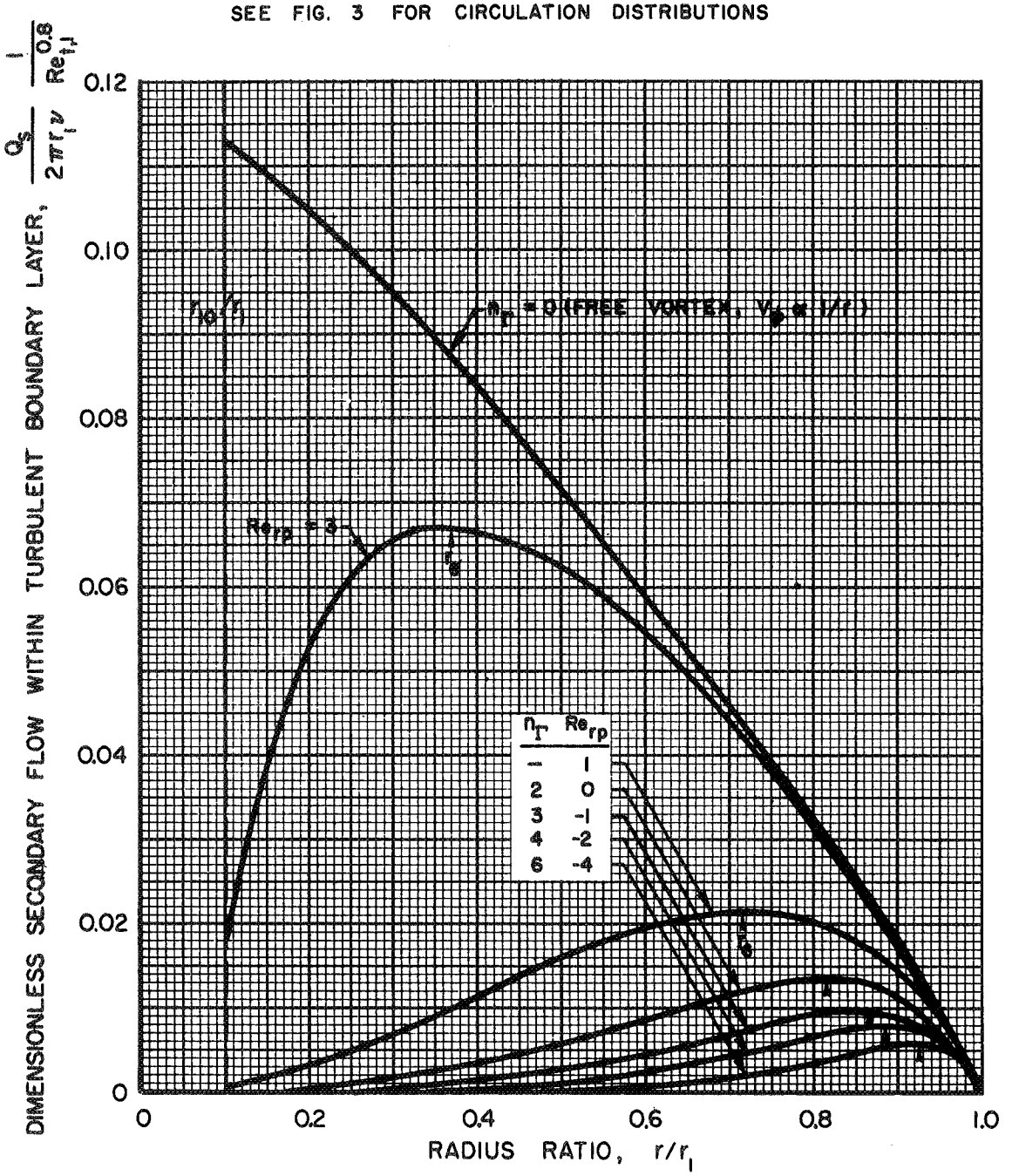

Figure 5

# VARIATION OF DIMENSIONLESS BOUNDARY LAYER THICKNESS WITH RADIUS FOR SEVERAL PRIMARY-FLOW CIRCULATION DISTRIBUTIONS

RESULTS DETERMINED FROM COMPUTATIONAL PROGRAM DISCUSSED IN REF. 4

SEE FIG. 4 FOR VARIATION OF SECONDARY-FLOW RATE WITH RADIUS

SEE FIG. 3 FOR CIRCULATION DISTRIBUTIONS

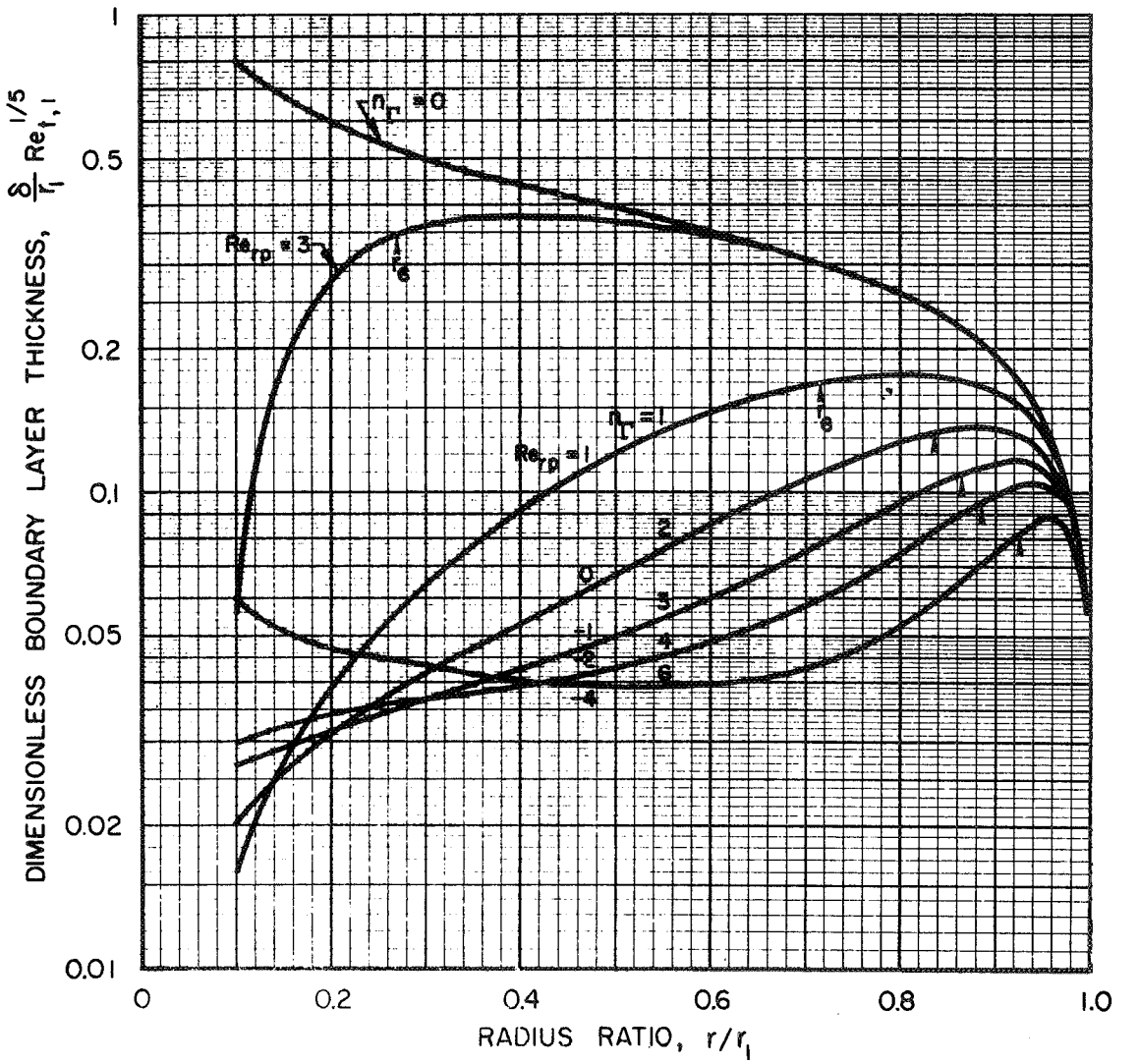

Figure 6



# VARIATION OF CIRCULATION GRADIENT AT OUTSIDE OF SECONDARY-FLOW CONTROL REGION WITH RADIAL REYNOLDS NUMBER

RESULTS DETERMINED FROM COMPUTATIONAL PROGRAM DISCUSSED IN REF. 3

CALCULATED ASSUMING $\bar{\Gamma} = R^{n_r}$ WHERE $n_r = 2 - Re_{rp}$

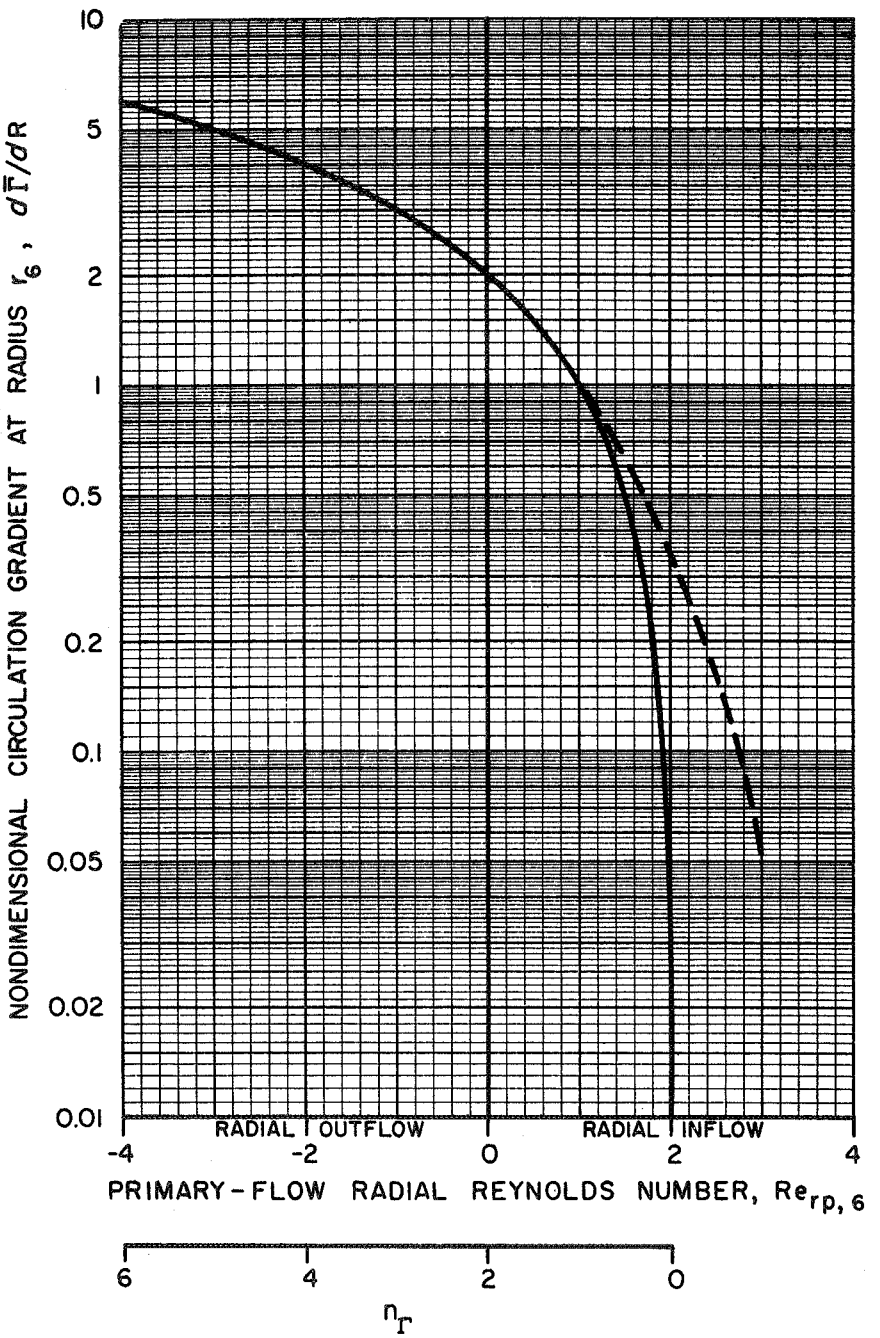

Figure 7

# EFFECT OF CIRCULATION DISTRIBUTION ON THE REQUIRED VARIATION OF END-WALL SKIN-FRICTION COEFFICIENT WITH RADIUS

REQUIRED FRICTION DETERMINED TO PROVIDE $U_{z,\delta} = 0$ ($Re_{r_p}$ = CONSTANT)

——— CALCULATED ASSUMING $\bar{\Gamma} = R^{n_\Gamma}$ WHERE $n_\Gamma = 2 - Re_{r_p}$ (SEE FIGS. 3 AND 6)

— — — CALCULATED USING RESULTS DETERMINED FROM COMPUTATIONAL PROGRAM DISCUSSED IN REF. 3 (SEE FIGS. 3 AND 6)

CONSTANT-DENSITY FLUID

$$\frac{C_{ft}}{C_{ft,6}} = \frac{\bar{\Gamma}^{-2}(d\bar{\Gamma}/dR)}{(d\bar{\Gamma}/dR)_{r_6}}$$

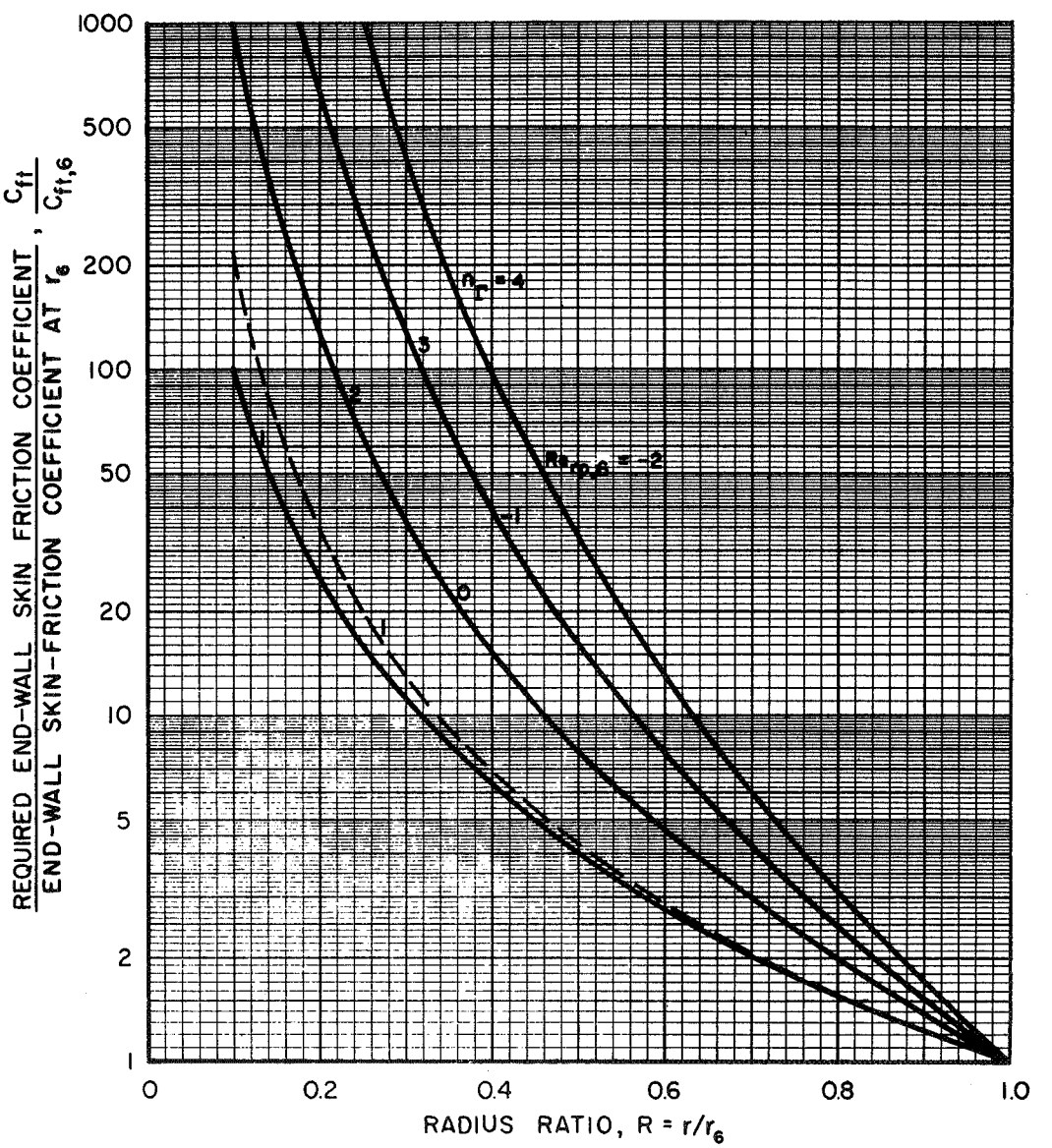

Figure 8

# EFFECT OF BOUNDARY LAYER CHARACTERISTICS AT $r_6$ ON THE VARIATION OF BOUNDARY LAYER THICKNESS WITH RADIUS WHEN USING DISTRIBUTED-FRICTION END WALLS

$C_{ft} / C_{ft,6}$ DETERMINED FROM FIG. 7 FOR $n_r$ = 2 (SOLID-BODY ROTATION)

$Re_{t,6}$ = 70,000 $r_6$ = 5 IN.

CONSTANT-DENSITY FLUID

| CURVE | DIMENSIONLESS QUANTITY OF FLOW IN BOUNDARY LAYER AT $r_6$, $S_6$ | REQUIRED VALUE OF FRICTION COEFFICIENT AT $r_6$, $C_{ft,6}$ | APPROXIMATE BOUNDARY LAYER THICKNESS, $\delta_6$, CORRESPONDING TO $S_6$ (SEE TEXT) |
|---|---|---|---|
| A | 1825 | 0.050 | 0.324 IN. |
| B | 730 | 0.020 | 0.176 IN. |
| C | 365 | 0.010 | 0.111 IN. |
| D | 183 | 0.005 | 0.070 IN. |

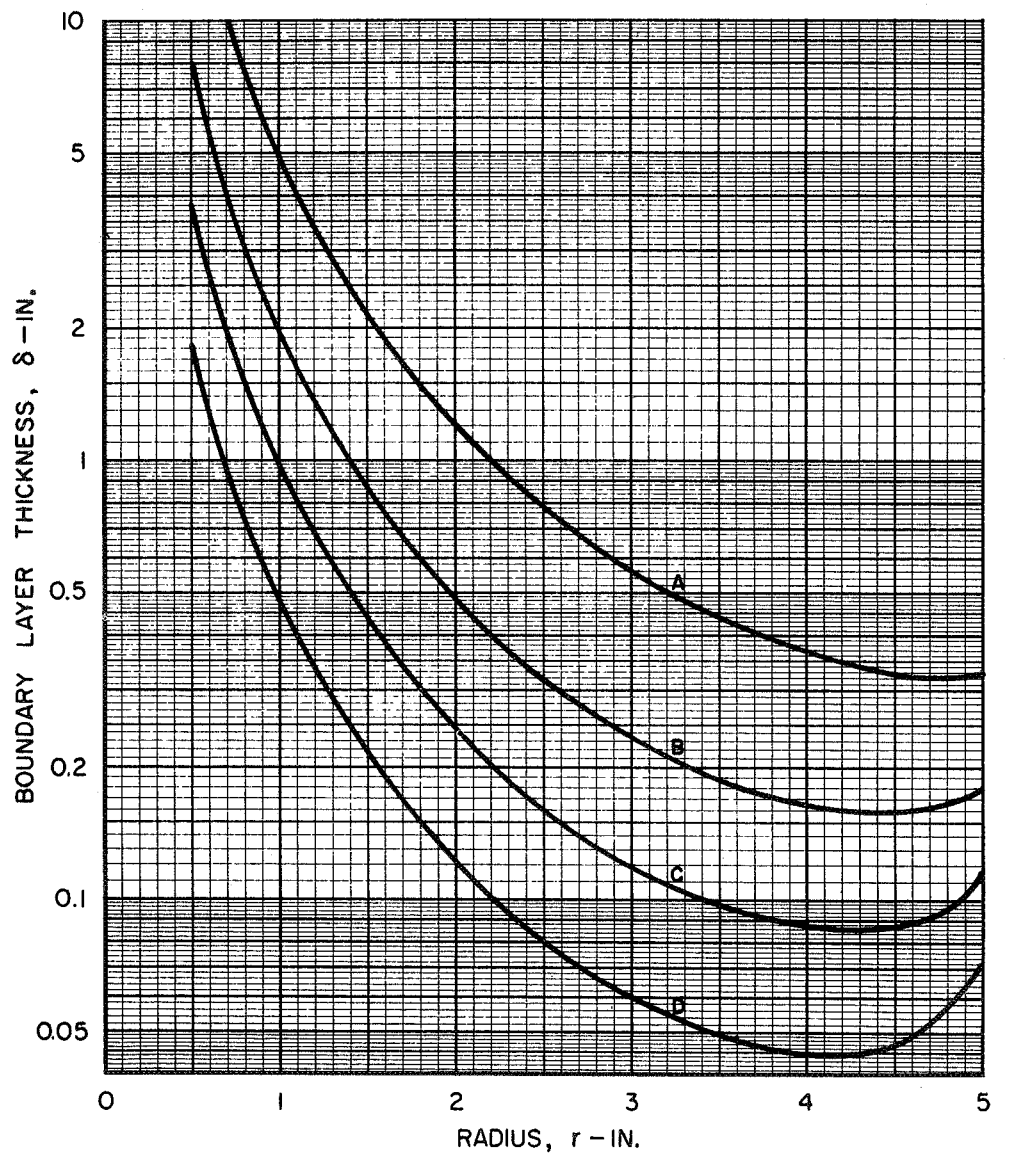

Figure 9

# EFFECT OF CIRCULATION DISTRIBUTION ON THE RADIAL VARIATION OF THE RATIO OF REQUIRED END-WALL SUCTION VELOCITY TO TANGENTIAL VELOCITY AT $r_6$

REQUIRED SUCTION VELOCITIES DETERMINED TO PROVIDE $U_{z,\delta} = 0$ WITH $U_{z,w} = 0$ AT $r_6$

$\bar{\Gamma} = R^{n_\Gamma}$ $\quad \xi/K_7 = 1.1$ $\quad K_7/C_{ff,0} = 160$

CONSTANT-DENSITY FLUID

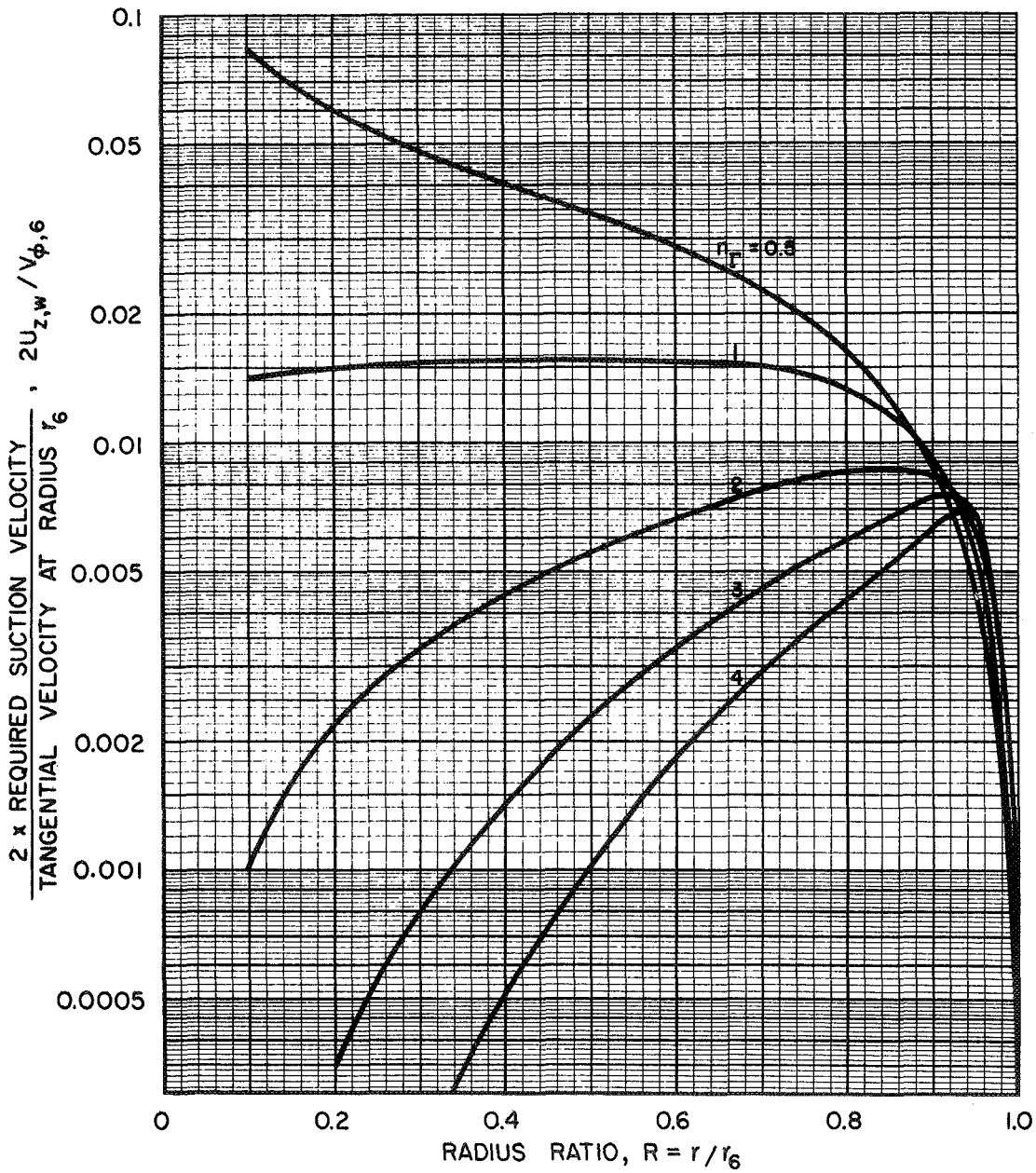

Figure 10

# EFFECT OF CIRCULATION DISTRIBUTION ON THE RADIAL VARIATION OF THE RATIO OF REQUIRED END-WALL SUCTION VELOCITY TO LOCAL TANGENTIAL VELOCITY

REQUIRED SUCTION VELOCITIES DETERMINED TO PROVIDE $U_{z,\delta} = 0$ WHEN $U_{z,w} = 0$ AT $r_6$

$$\bar{\Gamma} = R^{n_\Gamma}$$

$K_7 / C_{ft,0} = 160 \qquad \xi / K_7 = 1.1$

CONSTANT-DENSITY FLUID

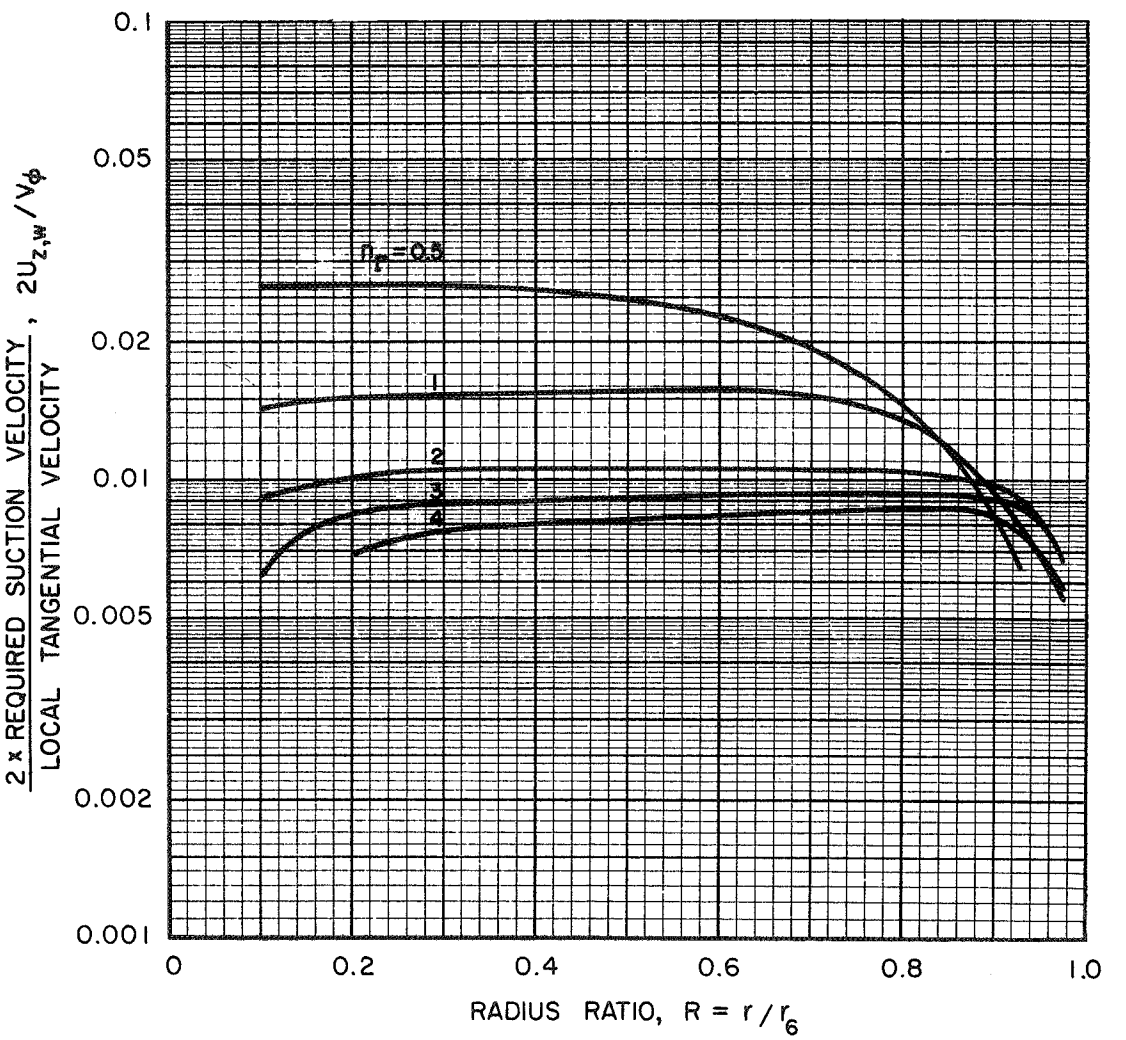

Figure 11

# EFFECT OF CIRCULATION DISTRIBUTION ON THE REQUIRED VARIATION OF SECONDARY FLOW WITH RADIUS WHEN USING DISTRIBUTED–SUCTION END WALLS

REFERENCE SECONDARY-FLOW RATE (DEFINED AT $r_6$) IS THAT FOR WHICH $U_{z,w} = 0$ AT $r_6$ AND IS PROPORTIONAL TO $1/(d\Gamma/dr)_{r_6}$

REQUIRED SUCTION VELOCITIES DETERMINED TO PROVIDE $U_{z,\delta} = 0$ FOR $R \leq 1$ (SEE FIGS. 9 AND 10)

$$\bar{\Gamma} = R^{n_\Gamma}$$

$$\xi/K_7 = 1.1$$

CONSTANT-DENSITY FLUID

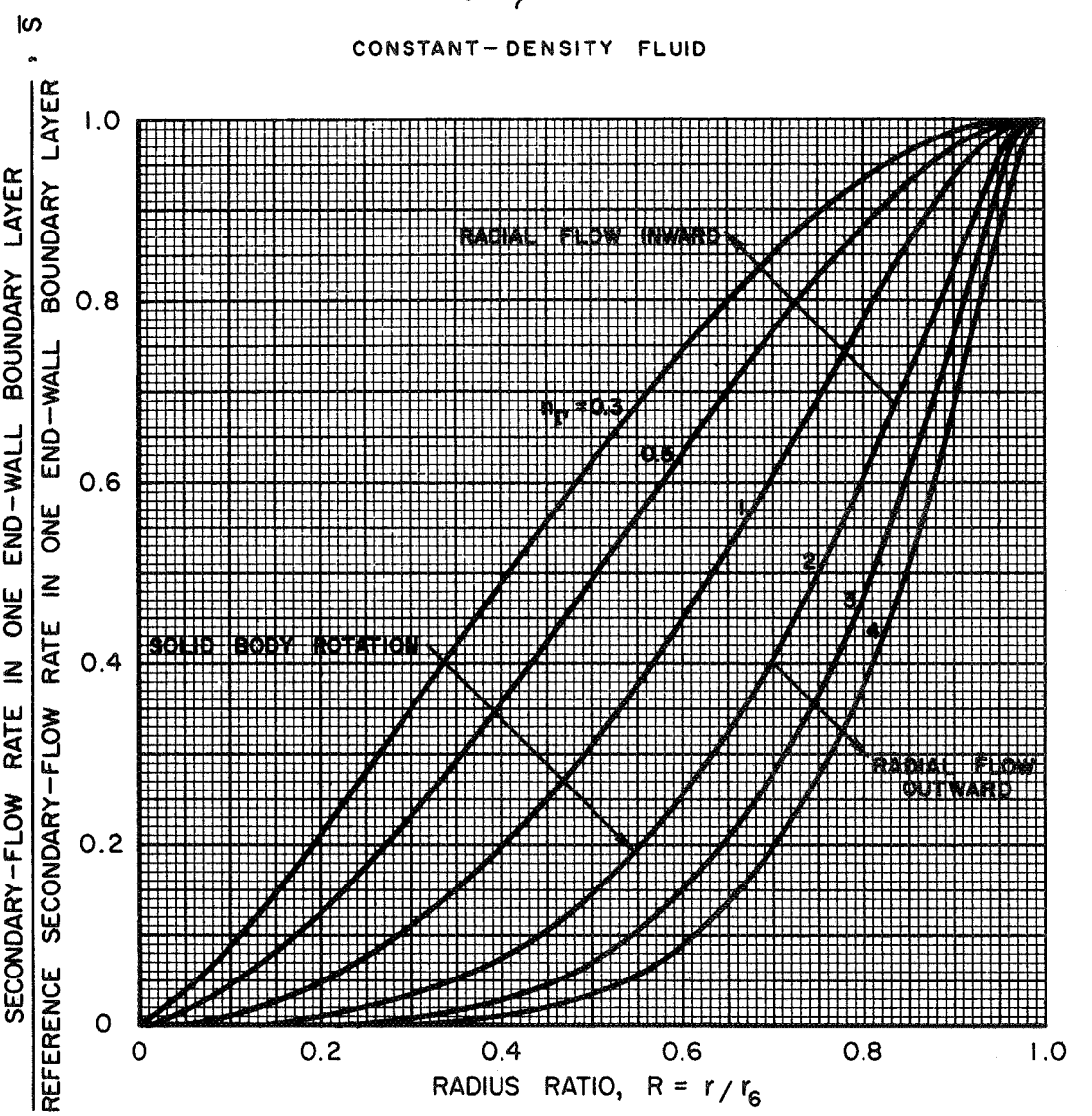

Figure 12

# EFFECT OF CIRCULATION DISTRIBUTION ON THE VARIATION OF BOUNDARY LAYER THICKNESS WITH RADIUS WHEN USING DISTRIBUTED-SUCTION END WALLS

WALL SUCTION VELOCITY RATIOS ARE SHOWN IN FIGS. 9 AND 10

$\bar{\Gamma} = R^{n_\Gamma}$

$Re_{t,e} = 70{,}000$ $\quad r_e = 5$ IN. $\quad C_{ft,o} = 0.005$

CONSTANT - DENSITY FLUID

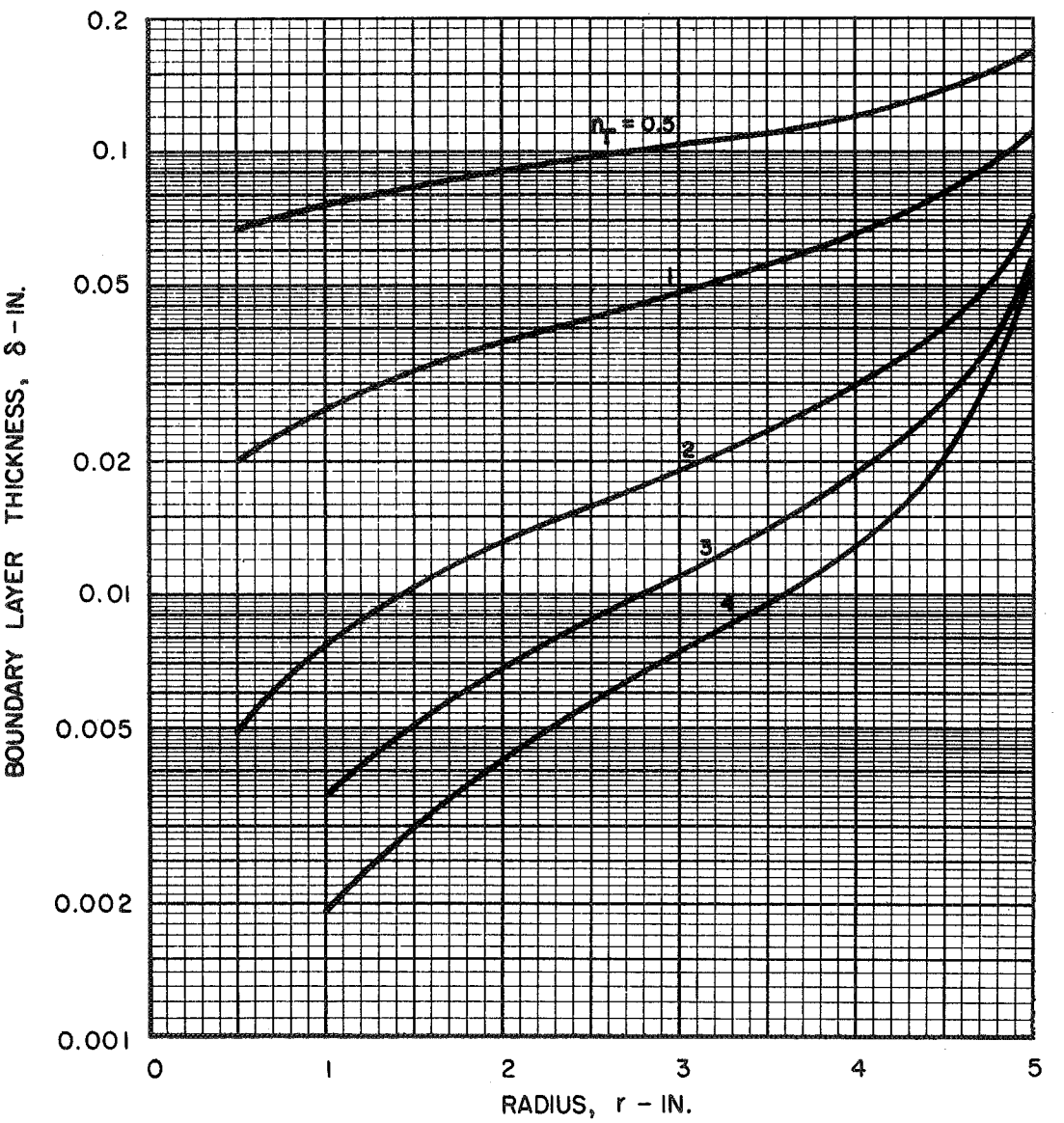

Figure 13

# EFFECT OF END-WALL SUCTION PARAMETER, $\xi/K_7$, ON THE VARIATION OF THE RATIO OF REQUIRED END-WALL SUCTION VELOCITY TO LOCAL TANGENTIAL VELOCITY

REQUIRED SUCTION VELOCITIES DETERMINED TO PROVIDE $U_{z,\delta} = 0$ WHEN $U_{z,w} = 0$ AT $r_6$

$\bar{r} = R^2$ (SOLID-BODY ROTATION) $K_7 / C_{ft,o} = 160$

CONSTANT-DENSITY FLUID

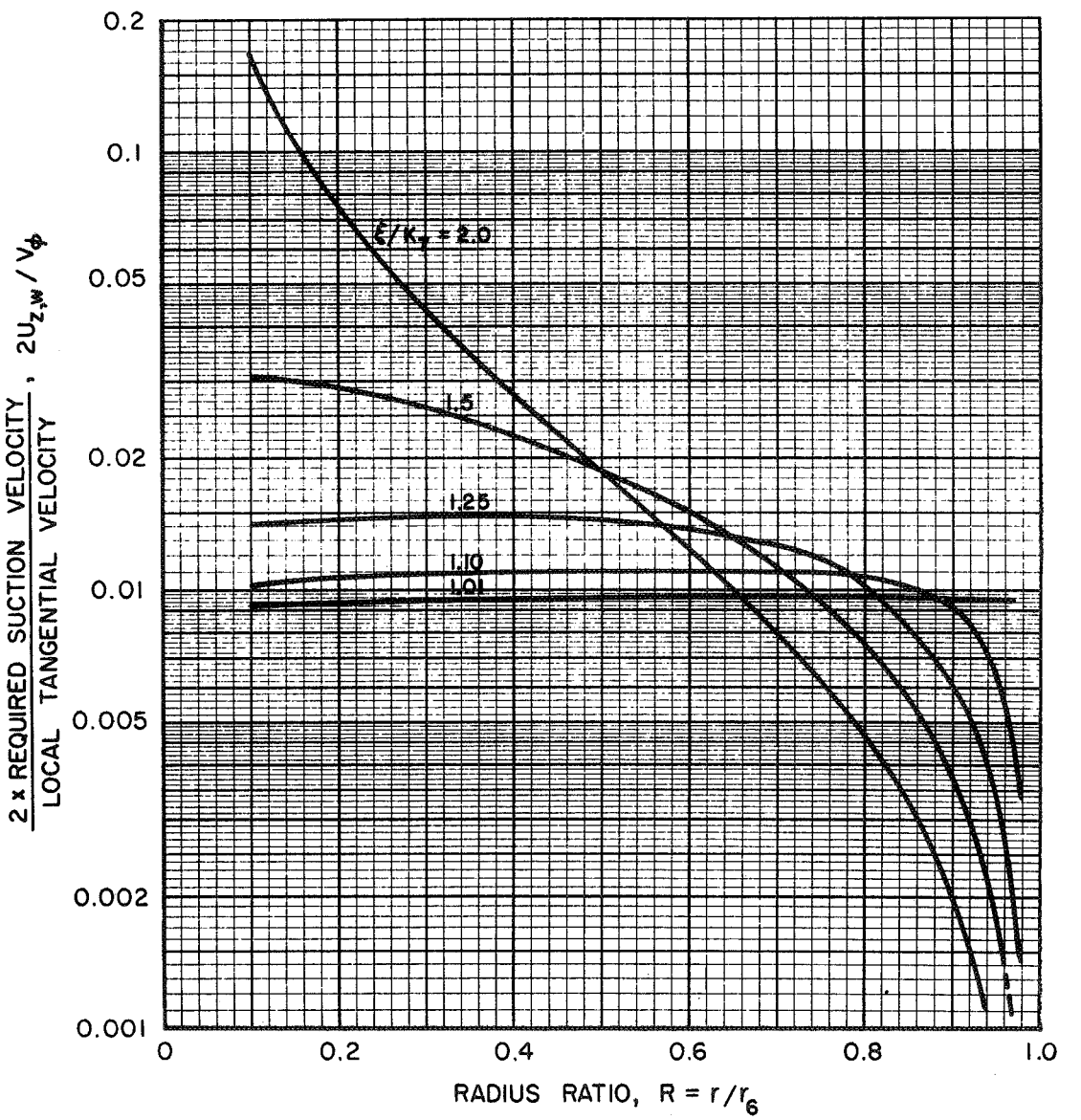

Figure 14



# EFFECT OF END-WALL SUCTION PARAMETER, $\xi/K_7$, ON THE REQUIRED VARIATION OF SECONDARY FLOW WITH RADIUS

REFERENCE SECONDARY-FLOW RATE (DEFINED AT $r_\delta$) IS THAT FOR WHICH $U_{z,w} = 0$ AT $r_\delta$ AND IS PROPORTIONAL TO $1/(d\Gamma/dr)\,r_\delta$

REQUIRED SUCTION VELOCITIES DETERMINED TO PROVIDE $U_{z,\delta} = 0$ FOR $R \leq 1$ (SEE FIG. 13)

$\bar{\Gamma} = R^2$ (SOLID-BODY ROTATION)

CONSTANT-DENSITY FLUID

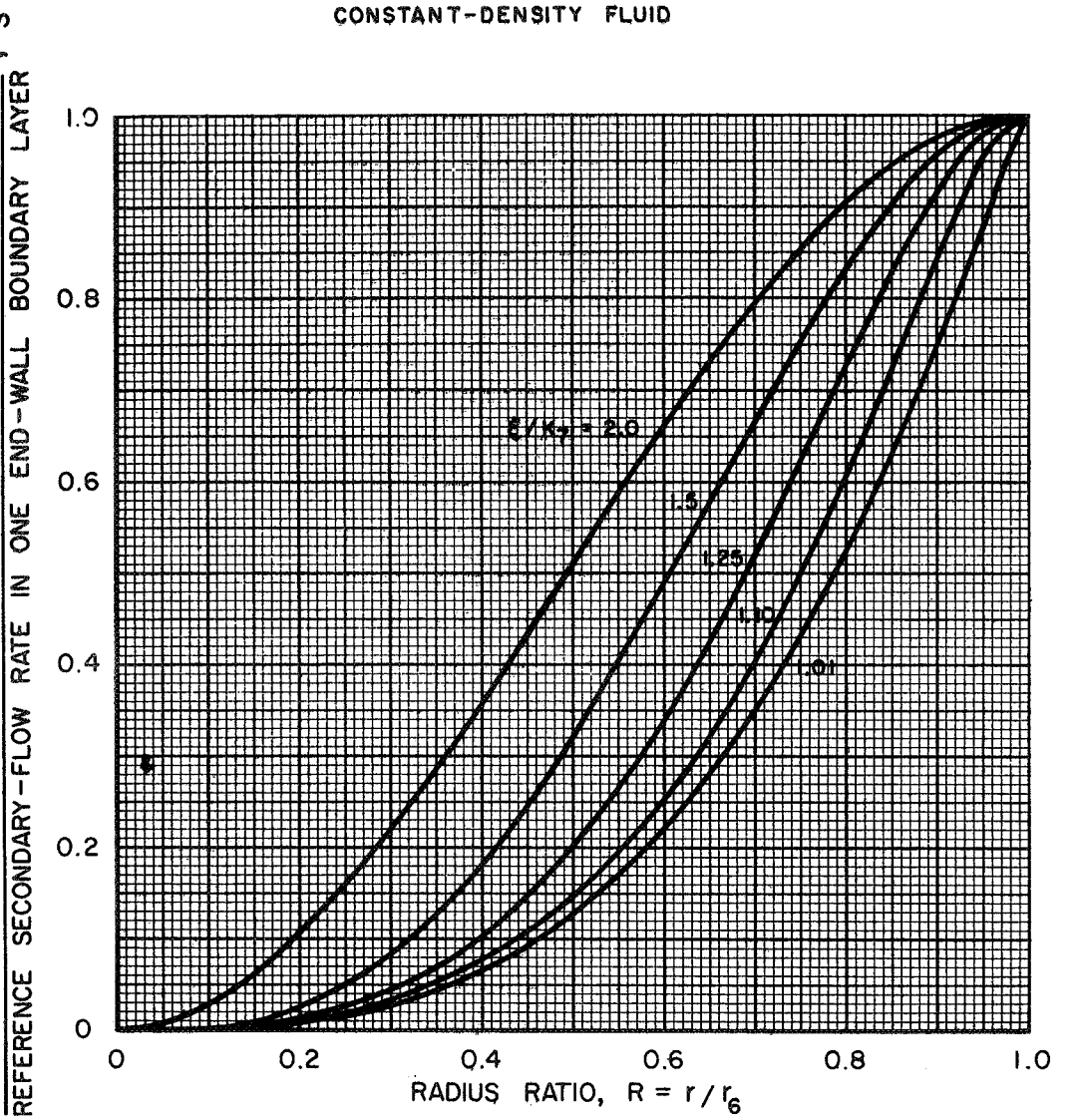

Figure 15

# EFFECT OF END-WALL SUCTION PARAMETER, $\epsilon/K_7$, ON THE VARIATION OF BOUNDARY LAYER THICKNESS WITH RADIUS

WALL SUCTION VELOCITY RATIOS ARE SHOWN IN FIG. 13

$\bar{\Gamma} = R^2$ (SOLID-BODY ROTATION)

$Re_{1,6} = 70{,}000$

$r_6 = 5$ IN. $\qquad C_{ff,o} = 0.005$

CONSTANT-DENSITY FLUID

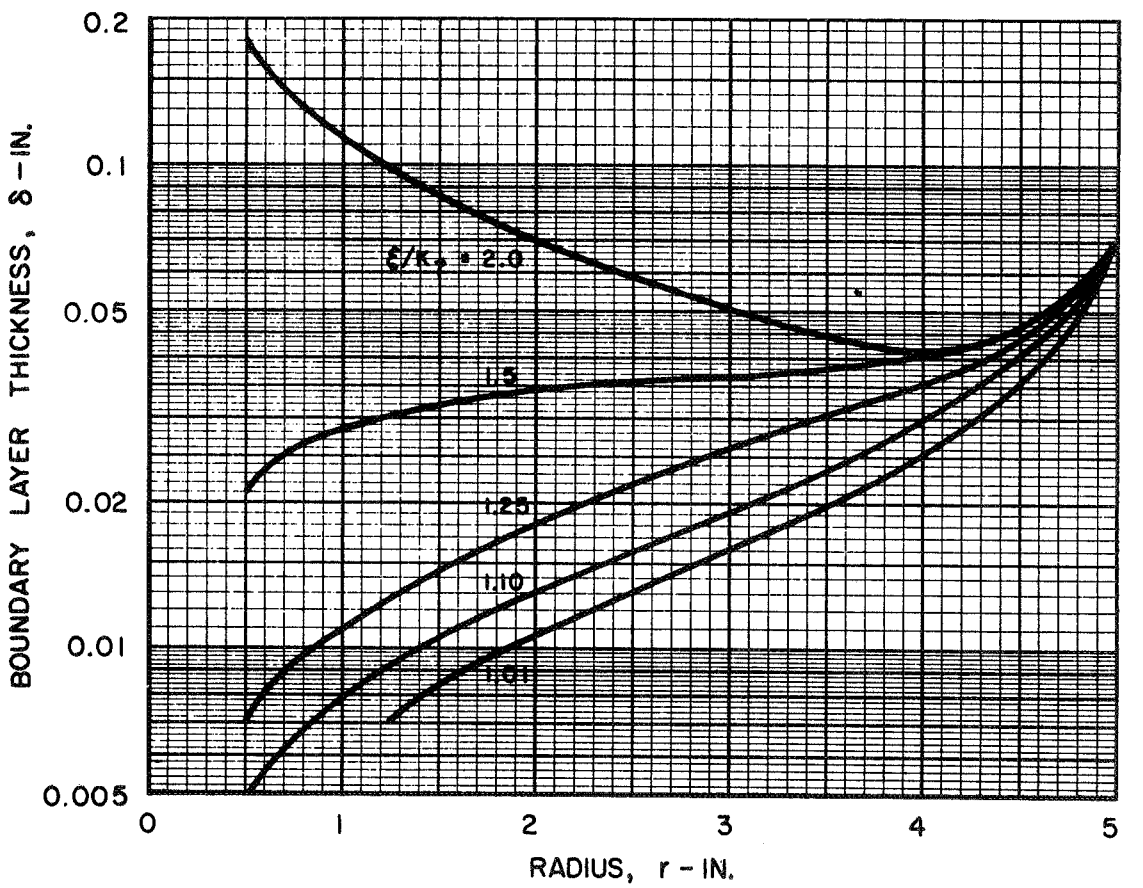

Figure 16

# EFFECT OF SECONDARY-FLOW RATE AT $r_6$ ON THE REQUIRED VARIATION OF SECONDARY-FLOW RATE WITH RADIUS WHEN USING DISTRIBUTED-SUCTION END WALLS

REFERENCE SECONDARY-FLOW RATE (DEFINED AT $r_6$) IS THAT FOR WHICH $U_{z,w} = 0$ AT $r_6$

REQUIRED SUCTION VELOCITIES DETERMINED TO PROVIDE $U_{z,\delta} = 0$ FOR $R \leq 1$

$\bar{\Gamma} = R^2$ (SOLID-BODY ROTATION) $\xi/K_7 = 1.1$

CONSTANT-DENSITY FLUID

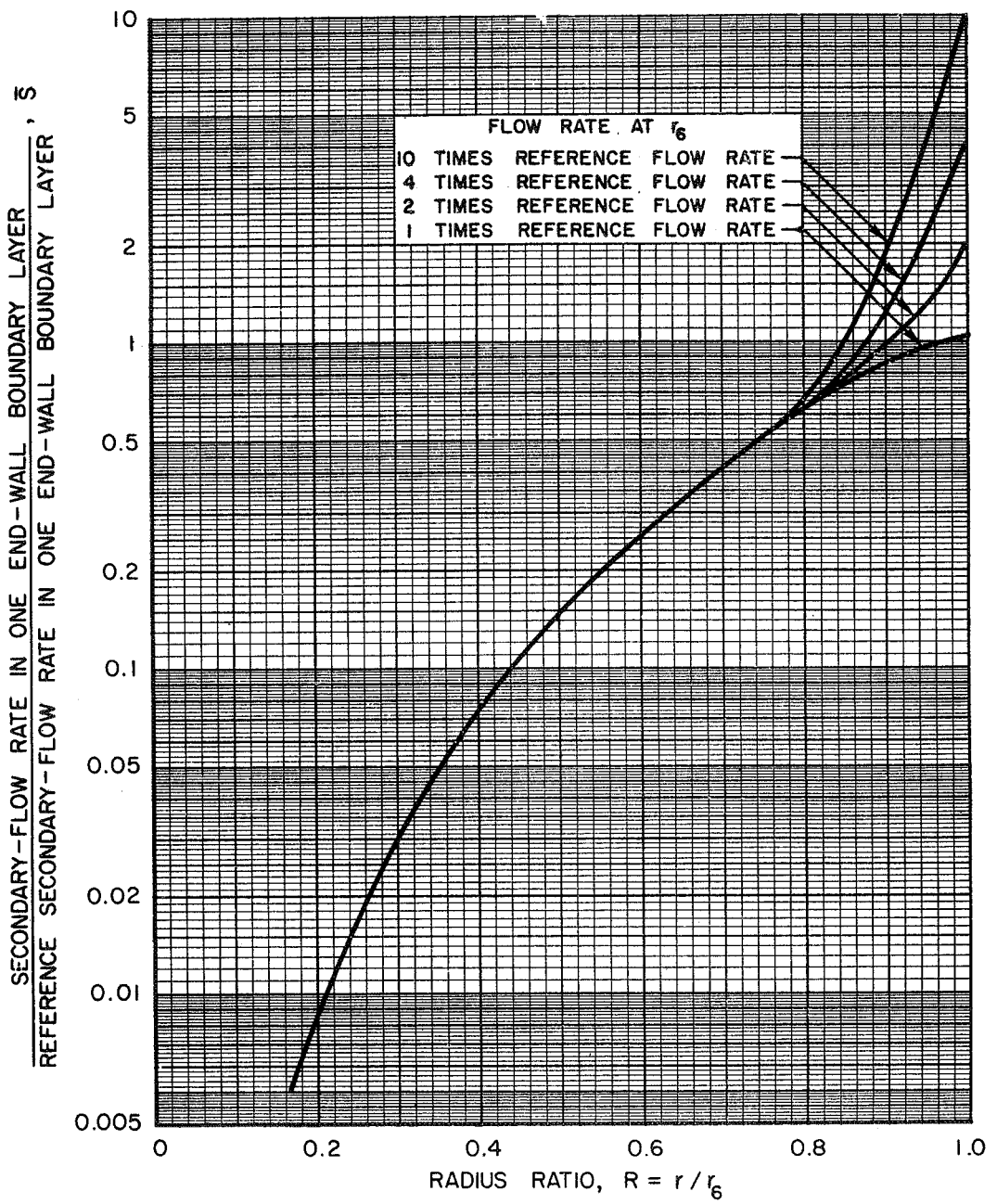

Figure 17

# EFFECT OF SECONDARY-FLOW RATE AT $r_6$ ON THE VARIATION OF BOUNDARY LAYER THICKNESS WITH RADIUS WHEN USING DISTRIBUTED-SUCTION END WALLS

REQUIRED VARIATION OF SECONDARY FLOW WITH RADIUS SHOWN ON FIG. 16

$\overline{\Gamma} = R^2$ (SOLID-BODY ROTATION)

$Re_{f,6} = 70{,}000$ $C_{ff,o} = 0.005$ $r_6 = 5$ IN.

CONSTANT-DENSITY FLUID

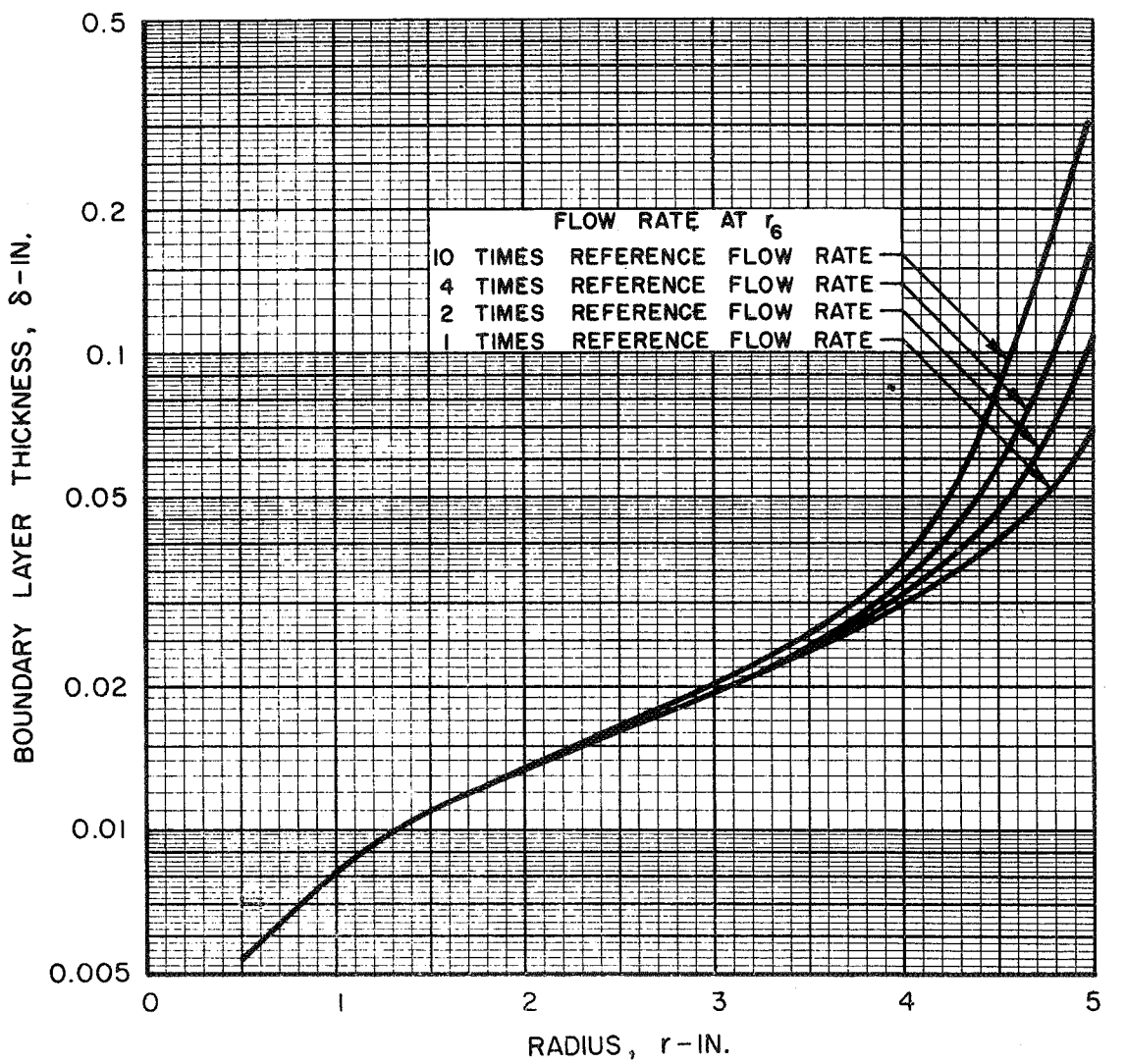

# EFFECT OF AXIAL-MASS-TRANSFER COEFFICIENT, $h_d$, ON THE VARIATION OF SECONDARY-FLOW-DENSITY RATIO WITH RADIUS WHEN USING DISTRIBUTED-FRICTION END WALLS

REQUIRED FRICTION DETERMINED TO PROVIDE $U_{z,\delta} = 0$

$\bar{\Gamma} = R^3$ $\qquad K_T / C_{f,t} = 160$

——— ASSUMED DENSITY DISTRIBUTION IN PRIMARY FLOW, $\bar{\rho}_p$

— — — CALCULATED DENSITY DISTRIBUTION IN SECONDARY FLOW, $\bar{\rho}_s$, FOR $h_d = G_1 V_\phi$

— — — CALCULATED DENSITY DISTRIBUTION IN SECONDARY FLOW, $\bar{\rho}_s$, FOR $h_d = G_2 V_{\phi,\delta}$

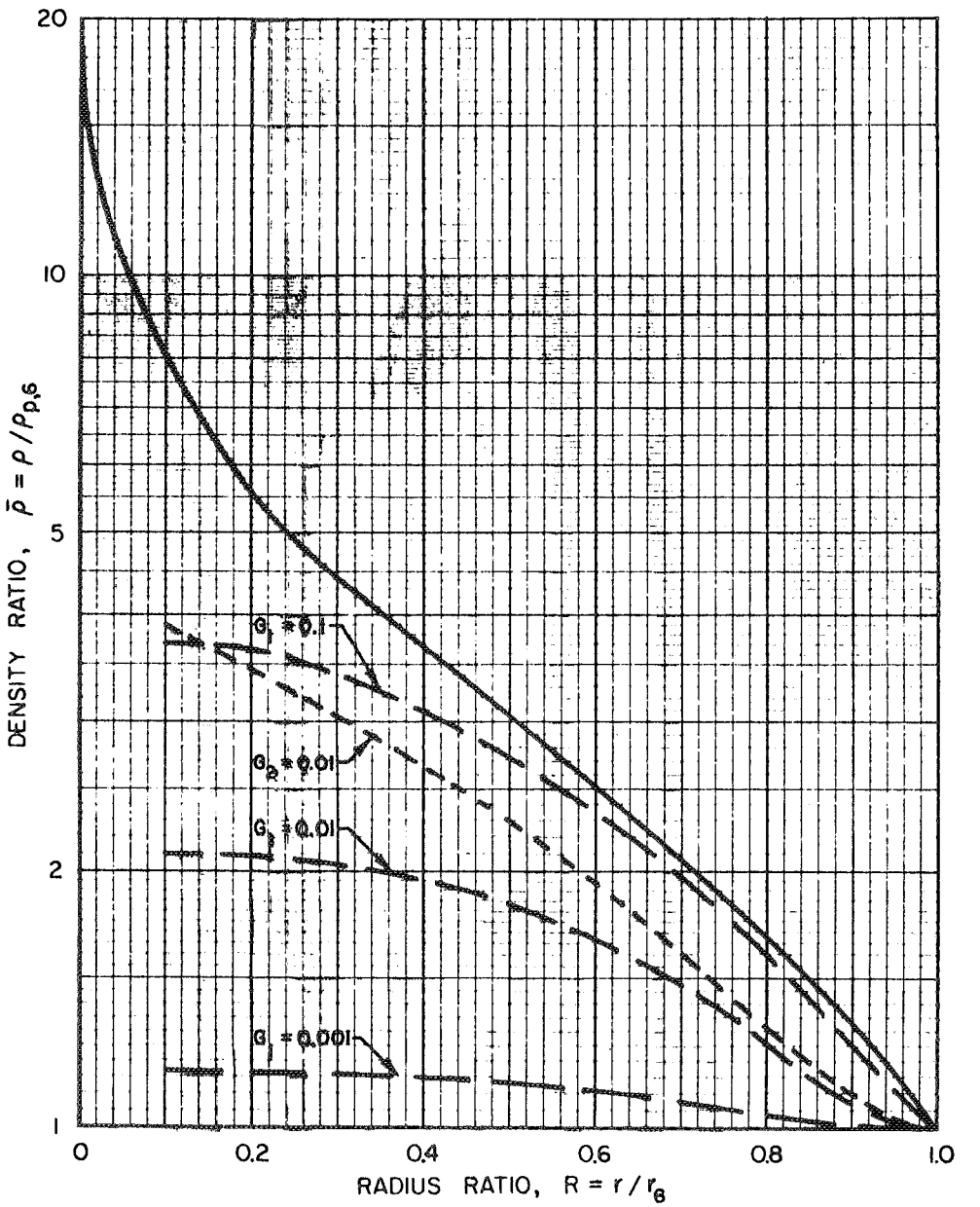

Figure 19

# EFFECT OF AXIAL-MASS-TRANSFER COEFFICIENT, $h_d$, ON THE REQUIRED VARIATION OF END-WALL SKIN-FRICTION COEFFICIENT RATIO WITH RADIUS

REQUIRED FRICTION DETERMINED TO PROVIDE $U_{z,\delta} = 0$

SEE FIG. 7 FOR REQUIRED CONSTANT-DENSITY FRICTION DISTRIBUTIONS

$\bar{\Gamma} = R^3$

$K_7 / C_{ff,6} = 160$

SEE FIG. 18 FOR DENSITY DISTRIBUTIONS

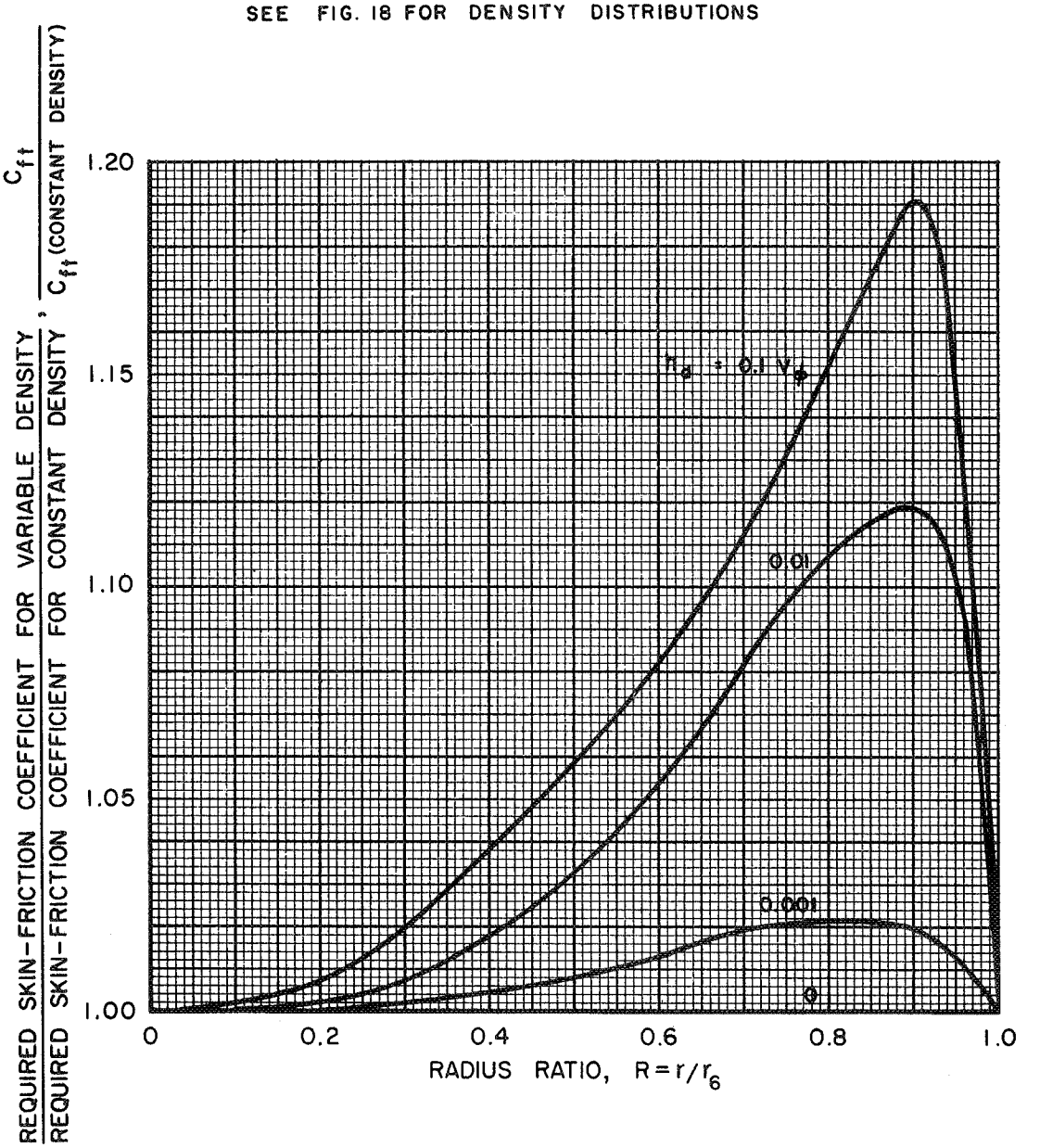

# EFFECT OF AXIAL-MASS-TRANSFER COEFFICIENT, $h_d$, ON THE VARIATION OF BOUNDARY LAYER THICKNESS WITH RADIUS WHEN USING DISTRIBUTED-FRICTION END WALLS

SEE FIG. 19 FOR REQUIRED DISTRIBUTED-FRICTION RATIO

$\bar{\Gamma} = R^3$

$Re_{t,6} = 70{,}000$ $r_6 = 5$ IN. $C_{ft,6} = 0.005$

SEE FIG. 18 FOR DENSITY DISTRIBUTIONS

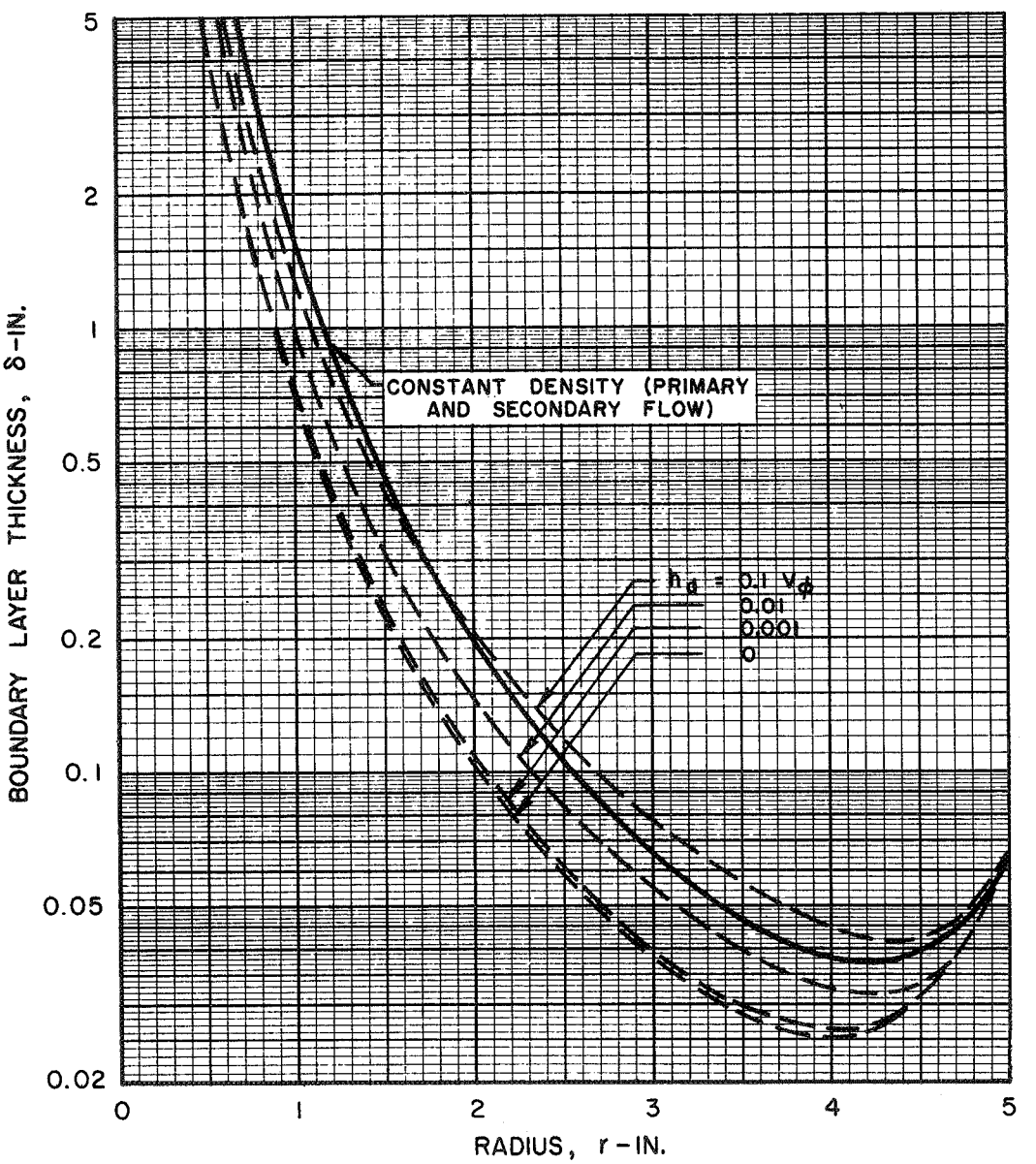

Figure 21

# VARIATION OF DIMENSIONLESS SECONDARY-FLOW TIME CONSTANT WITH AXIAL-MASS-TRANSFER PARAMETER WHEN USING DISTRIBUTED-FRICTION END WALLS

REQUIRED FRICTION DETERMINED TO PROVIDE $U_{z,\delta} = 0$

$\bar{r} = R^3$

$S_6 = 121$ $\qquad$ $L/r_6 = 6$

SEE FIG. 18 FOR TYPICAL DENSITY DISTRIBUTIONS

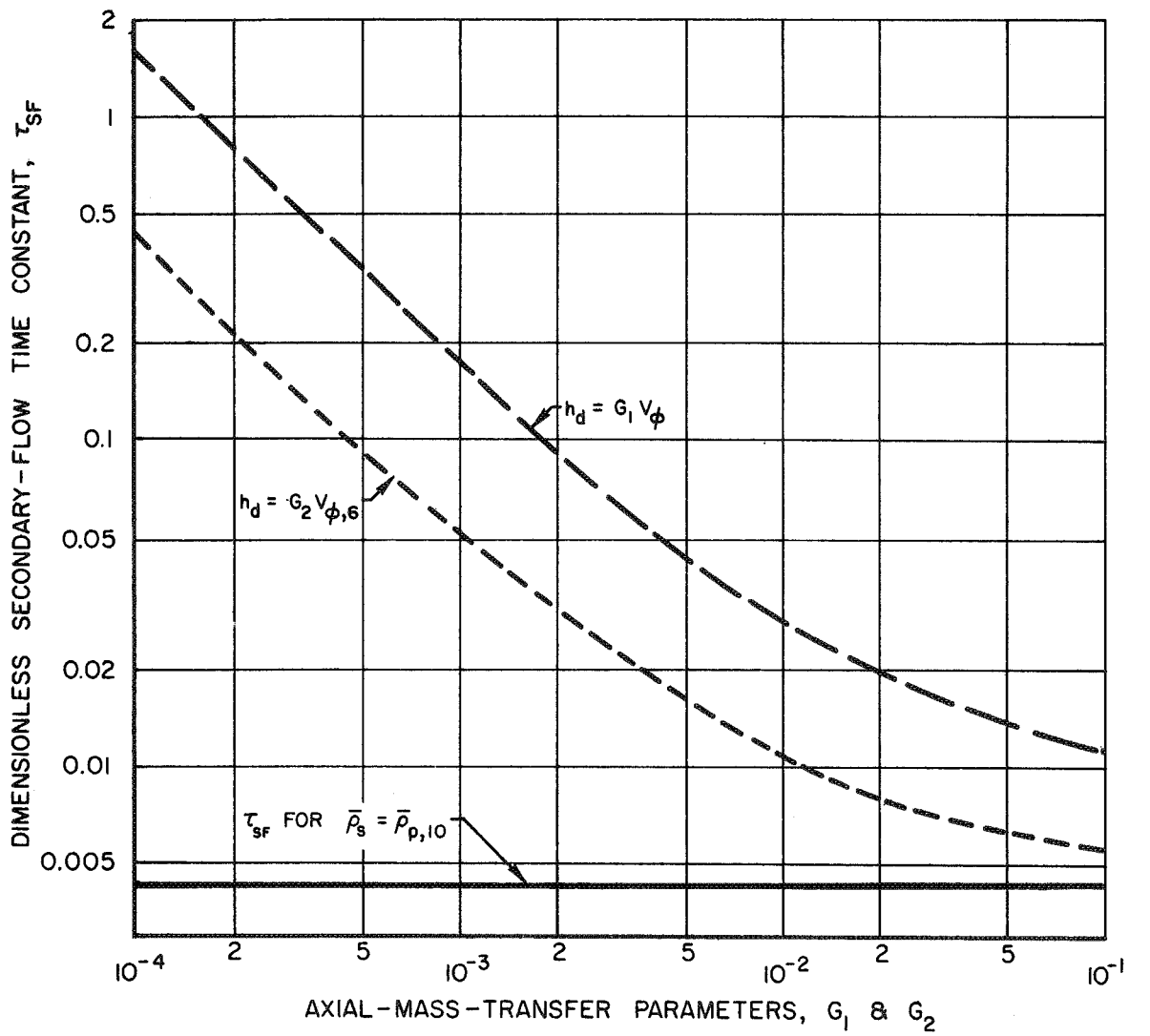

# EFFECT OF AXIAL-MASS-TRANSFER COEFFICIENT, $h_d$, ON THE VARIATION OF SECONDARY-FLOW-DENSITY RATIO WITH RADIUS WHEN USING DISTRIBUTED-SUCTION END WALLS

REQUIRED SUCTION VELOCITIES DETERMINED TO PROVIDE $U_{z,\delta} = 0$ WHEN $U_{z,w} = 0$ AT $r_\delta$

$\bar{\Gamma} = R^3$ $\quad K_7/C_{ft,o} = 160$ $\quad \xi/K_7 = 1.25$

ASSUMED DENSITY DISTRIBUTION IN PRIMARY FLOW, $\bar{\rho}_p$

CALCULATED DENSITY DISTRIBUTION IN SECONDARY FLOW, $\bar{\rho}_s$, FOR $h_d = G_1 V_\phi$

CALCULATED DENSITY DISTRIBUTION IN SECONDARY FLOW, $\rho_s$, FOR $h_d = G_2 V_\phi$

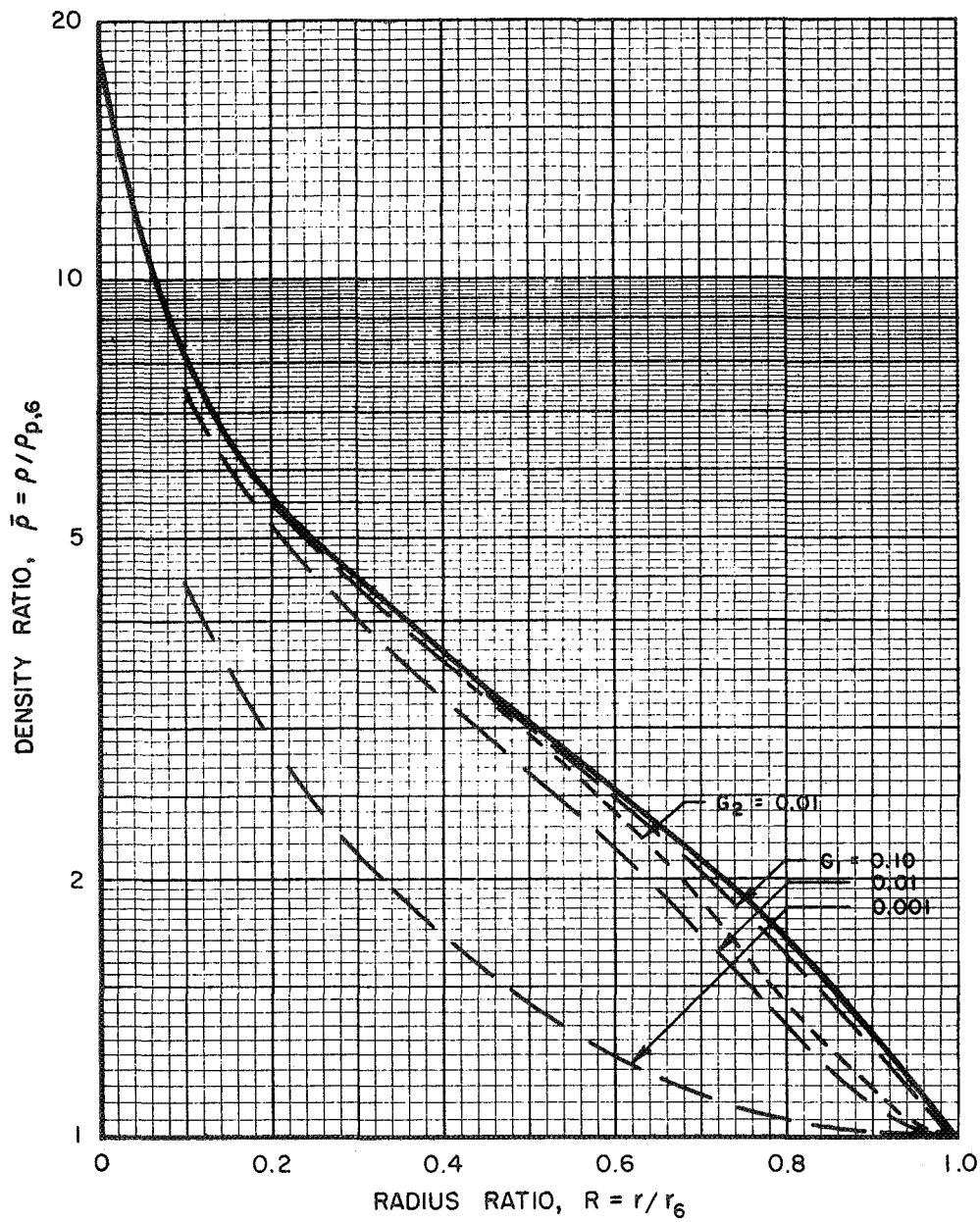

Figure 23

# EFFECT OF AXIAL-MASS-TRANSFER COEFFICIENT, $h_d$, ON THE REQUIRED VARIATION OF SECONDARY FLOW WITH RADIUS WHEN USING DISTRIBUTED-SUCTION END WALLS

REFERENCE SECONDARY FLOW RATE (DEFINED AT $r_6$) IS THAT FOR WHICH $U_{z,w} = 0$ AT $r_6$

REQUIRED SUCTION VELOCITIES DETERMINED TO PROVIDE $U_{z,\delta} = 0$ FOR $R \leq 1$

$\bar{\Gamma} = R^3$ $\quad K_7/C_{ft,o} = 160$ $\quad \xi/K_7 = 1.25$

SEE FIG. 22 FOR DENSITY DISTRIBUTIONS

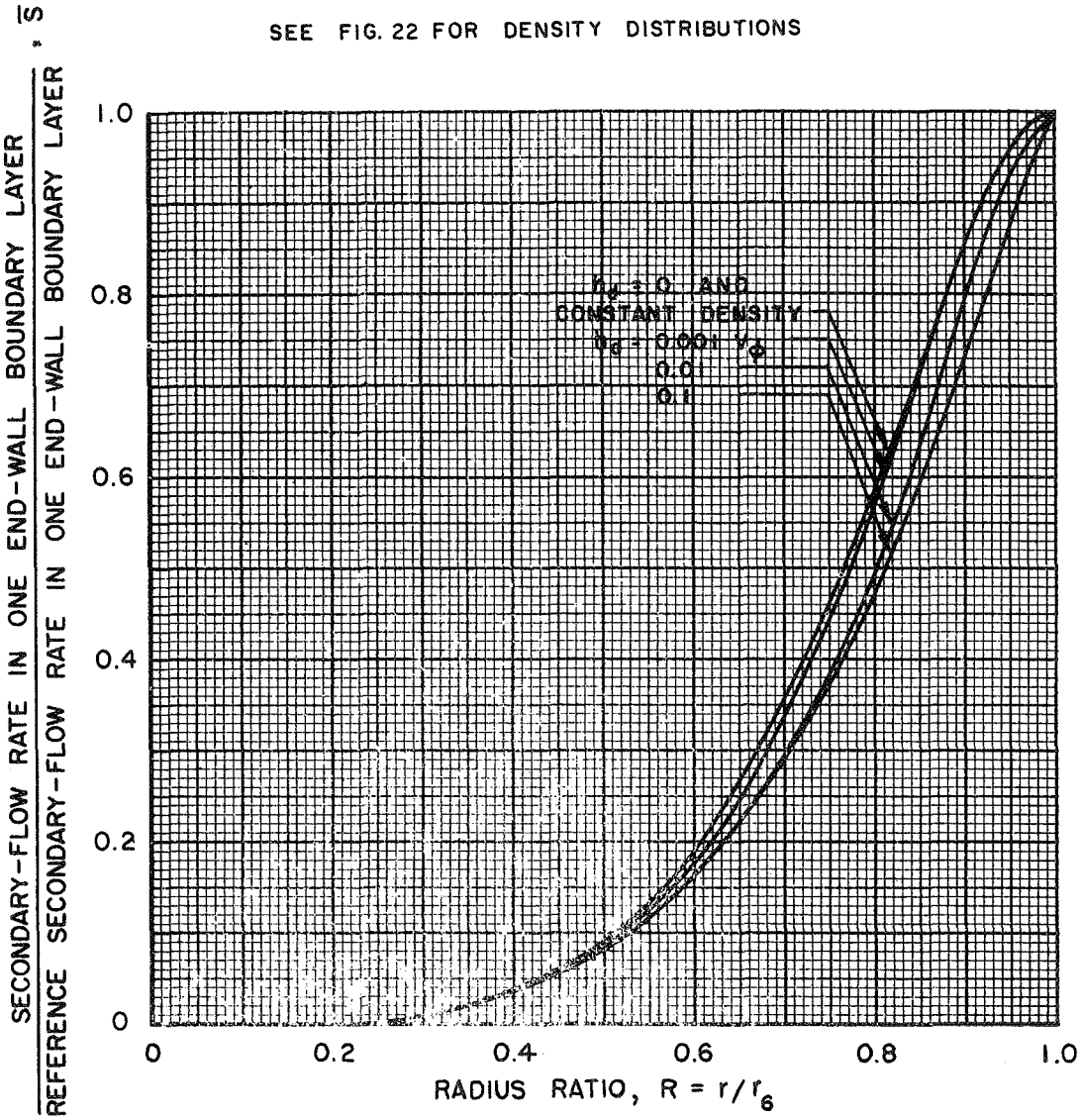

Figure 24

# EFFECT OF AXIAL-MASS-TRANSFER COEFFICIENT, $h_d$, ON THE VARIATION OF BOUNDARY LAYER THICKNESS WITH RADIUS WHEN USING DISTRIBUTED-SUCTION END WALLS

REQUIRED VARIATION OF SECONDARY FLOW WITH RADIUS SHOWN ON FIG. 23

$\bar{\Gamma} = R^3$

$Re_{t,6} = 70{,}000$

$C_{ft,6} = 0.005 \qquad s_6 = 121 \qquad r_6 = 5$ IN.

SEE FIG. 22 FOR DENSITY DISTRIBUTIONS

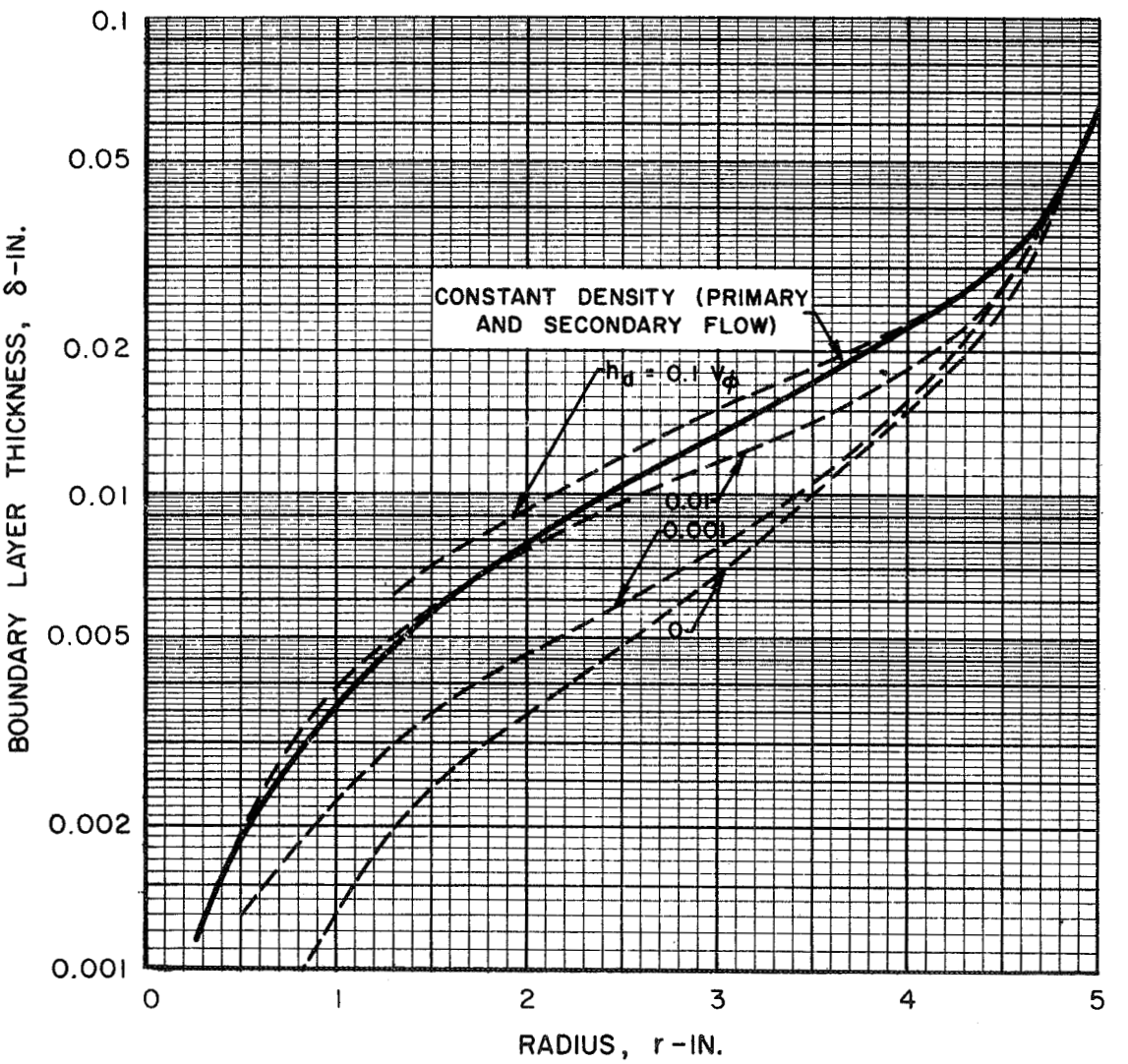

Figure 25

# VARIATION OF DIMENSIONLESS SECONDARY-FLOW TIME CONSTANT WITH AXIAL-MASS-TRANSFER PARAMETER WHEN USING DISTRIBUTED-SUCTION END WALLS

REQUIRED SUCTION VELOCITIES DETERMINED TO PROVIDE $U_{z,\delta} = 0$ WHEN $U_{z,w} = 0$ AT $r_6$

SEE FIG. 23 FOR TYPICAL REQUIRED VARIATION OF SECONDARY FLOW WITH RADIUS

$\bar{\Gamma} = R^3$

$\xi/K_7 = 1.25$ $\quad L/r_6 = 6$ $\quad S_6 = 121$

SEE FIG. 22 FOR TYPICAL DENSITY DISTRIBUTIONS

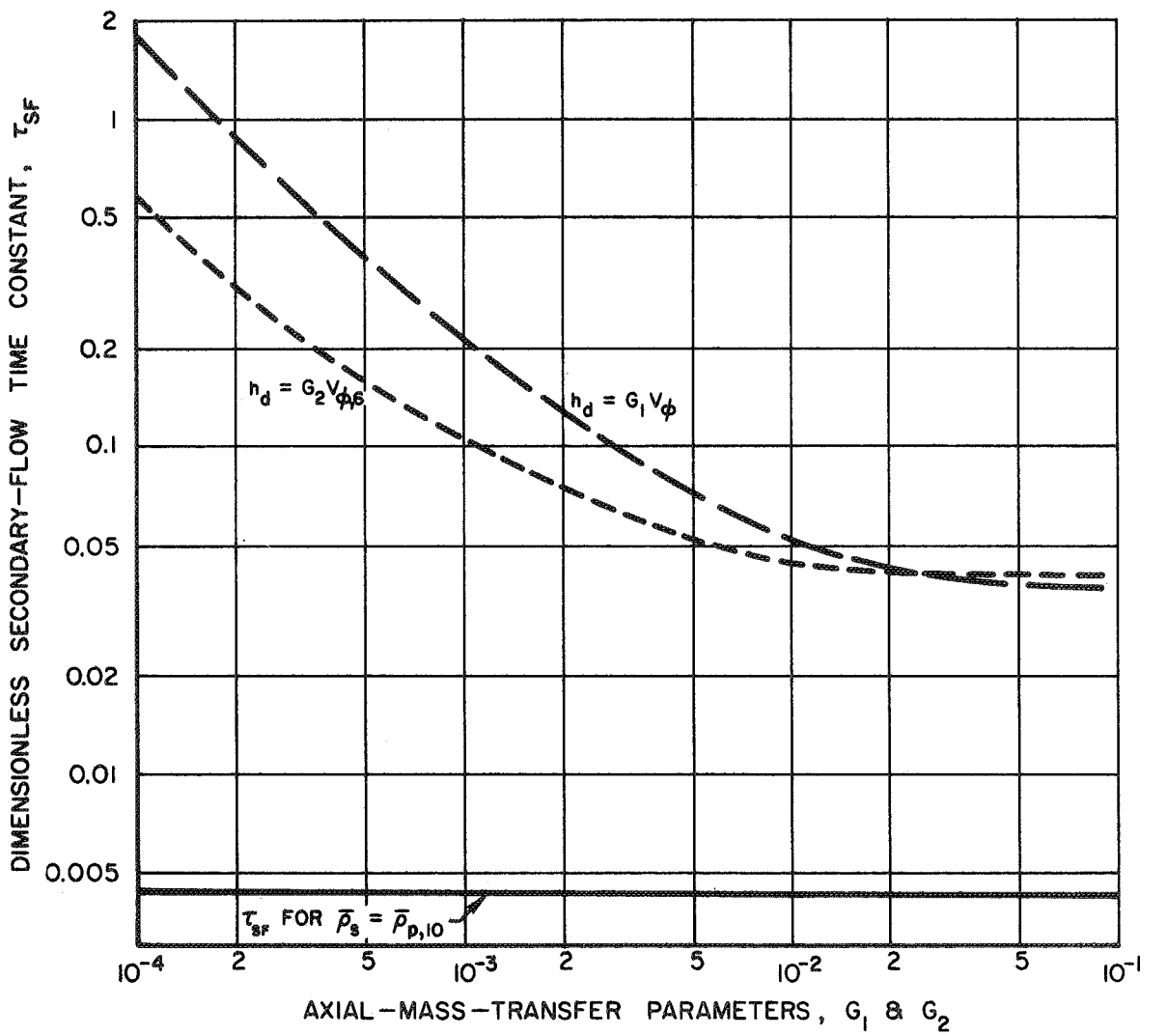

FLOW MODEL FOR AXIAL MASS TRANSFER

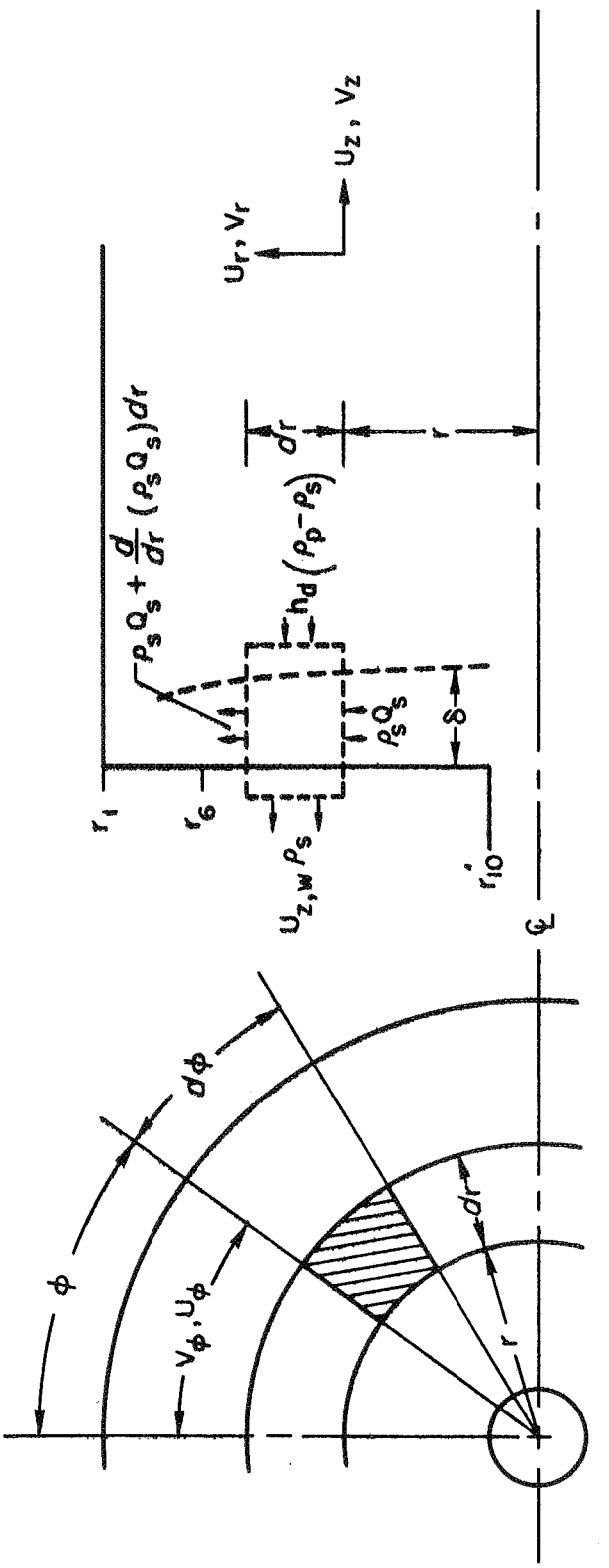

UNCLASSIFIED
CONFIDENTIAL

*"The aeronautical and space activities of the United States shall be conducted so as to contribute . . . to the expansion of human knowledge of phenomena in the atmosphere and space. The Administration shall provide for the widest practicable and appropriate dissemination of information concerning its activities and the results thereof."*

—National Aeronautics and Space Act of 1958

# NASA SCIENTIFIC AND TECHNICAL PUBLICATIONS

**TECHNICAL REPORTS:** Scientific and technical information considered important, complete, and a lasting contribution to existing knowledge.

**TECHNICAL NOTES:** Information less broad in scope but nevertheless of importance as a contribution to existing knowledge.

**TECHNICAL MEMORANDUMS:** Information receiving limited distribution because of preliminary data, security classification, or other reasons.

**CONTRACTOR REPORTS:** Technical information generated in connection with a NASA contract or grant and released under NASA auspices.

**TECHNICAL TRANSLATIONS:** Information published in a foreign language considered to merit NASA distribution in English.

**TECHNICAL REPRINTS:** Information derived from NASA activities and initially published in the form of journal articles.

**SPECIAL PUBLICATIONS:** Information derived from or of value to NASA activities but not necessarily reporting the results of individual NASA-programmed scientific efforts. Publications include conference proceedings, monographs, data compilations, handbooks, sourcebooks, and special bibliographies.

*Details on the availability of these publications may be obtained from:*

SCIENTIFIC AND TECHNICAL INFORMATION DIVISION

NATIONAL AERONAUTICS AND SPACE ADMINISTRATION

Washington, D.C. 20546

UNCLASSIFIED
CONFIDENTIAL